



Theses and Dissertations

---

2005-06-22

## Assessment of Cell Death Parameters in Bovine Parvovirus-Infected EBTr Cells

Lubna Salah Eldin Abdel Latif  
*Brigham Young University - Provo*

Follow this and additional works at: <https://scholarsarchive.byu.edu/etd>



Part of the [Microbiology Commons](#)

---

### BYU ScholarsArchive Citation

Latif, Lubna Salah Eldin Abdel, "Assessment of Cell Death Parameters in Bovine Parvovirus-Infected EBTr Cells" (2005). *Theses and Dissertations*. 445.

<https://scholarsarchive.byu.edu/etd/445>

This Thesis is brought to you for free and open access by BYU ScholarsArchive. It has been accepted for inclusion in Theses and Dissertations by an authorized administrator of BYU ScholarsArchive. For more information, please contact [scholarsarchive@byu.edu](mailto:scholarsarchive@byu.edu), [ellen\\_amatangelo@byu.edu](mailto:ellen_amatangelo@byu.edu).

ASSESSMENT OF CELL DEATH PARAMETERS IN BOVINE  
PARVOVIRUS-INFECTED EBTr CELLS

by

Lubna S. Abdel-Latif

A thesis submitted to the faculty of

Brigham Young University

in partial fulfillment of the requirements for the degree of

Master of Science

Department of Microbiology and Molecular Biology

Brigham Young University

August 2005

BRIGHAM YOUNG UNIVERSITY

GRADUATE COMMITTEE APPROVAL

of a thesis submitted by

Lubna S. Abdel-Latif

This thesis has been read by each member of the following graduate committee and by majority vote has been found to be satisfactory.

\_\_\_\_\_  
Date

\_\_\_\_\_  
F. Brent Johnson, Chair

\_\_\_\_\_  
Date

\_\_\_\_\_  
Byron K. Murray

\_\_\_\_\_  
Date

\_\_\_\_\_  
Kim L. O'Neill

BRIGHAM YOUNG UNIVERSITY

As chair of the candidate's graduate committee, I have read the thesis of Lubna S. Abdel-Latif in its final form and have found that (1) its format, citations, and bibliographical style are consistent and acceptable and fulfill university and department style requirements; (2) its illustrative materials including figures, tables, and charts are in place; and (3) the final manuscript is satisfactory to the graduate committee and is ready for submission to the university library.

---

Date

---

F. Brent Johnson  
Chair, Graduate Committee

Accepted for the Department

---

Laura Bridgewater  
Graduate Coordinator

Accepted for the College

---

R. Kent Crookston  
Dean, College of Biology and Agriculture

## ABSTRACT

### ASSESSMENT OF CELL DEATH PARAMETERS IN BOVINE PARVOVIRIS- INFECTED EBTr CELLS

Lubna S. Abdel-Latif

Department of Microbiology and Molecular Biology

Master of Science

Bovine parvovirus (BPV) is a helper-independent parvovirus. It has a small icosahedral capsid with a single stranded DNA genome. It is a highly stable virus with a narrow host range. It causes acute gastroenteritis in calves. It is considered to be a cytolytic virus because it kills the host cells. However, the mechanism by which the virus causes cell death is not known. The work described in this thesis assessed different parameters of cell death in BPV infected embryonic bovine tracheal (EBTr) cells.

There are several ways for viruses to induce cell death. Viruses can induce apoptosis in the infected cell. They can also kill the host cell by necrosis. Several approaches were used in this work to look for evidence of apoptosis and necrosis. Cells undergoing apoptosis exhibit cardinal signs that distinguish them from other dying cells. Among these signs are the exposure of phosphatidylserine to the outer surface of the

plasma membrane, DNA fragmentation into non-random DNA sections that are multimers of 180bp, nuclear morphology changes and caspase activation. These signs were studied in this research and data collected from these experiments did not show any positive sign of apoptosis in infected cells due to virus infection.

Cells undergoing a necrotic cell death have a different pattern. The cells swell then burst releasing their cytoplasmic contents. The DNA is fragmented in a random fashion. Cellular morphology was studied in this research and the data suggested that BPV infected cells swell, then shrink and detach from the surface of the culture vessel. Moreover, formation of apoptotic bodies was not detected in dying infected cells. Release of cytoplasmic contents was also assessed by looking at concentrations of LDH enzyme, viral haemagglutinin, and the number of infectious viral particles in the media of infected cells. Data from the different approaches employed in this study do not support the hypothesis that BPV kills the infected EBTr cell by apoptosis, rather, infected cells in culture become necrotic, swell, release their cytoplasmic contents, and detach.

## ACKNOWLEDGMENTS

I would like to express my appreciation for the BYU Jerusalem Center for Near Eastern Studies for giving me and other Palestinian students the opportunity to come to BYU and improve ourselves. I would also like to thank Dr. Cecil Clark for choosing me to get this scholarship. I would also like to thank my committee members; Dr. Johnson, Dr. Murray and Dr. O'Neill for being there anytime I had a question or needed help.

Mum and Dad, thanks for lightening my life with your love and guidance. You have been so supportive to every decision I make, especially this one, although I know how hard it was on you to accept the fact that I will not be living with you for two years. But it was you who taught me to do the right thing for my country, and at this time getting myself educated is the only thing that I can give to my country and people, hoping that I will try to give more in the coming future. Fadi, thanks for all the love and support that you gave me. Fida', thanks for being the good sister and the best friend you are. Montasser, your presence makes life easier because you are always smiling and optimistic, thanks for being such a good brother. I would like to express all the appreciation to grandpa, grandma and aunt Wafa for teaching me all the good morals that makes me who I am today.

My friends Seiga, Staci, Tuleen and Hilda, thanks so much for making my staying in the U.S easier. Thanks to Becki and Enkhmart in Dr. Johnson's lab for all the help in the lab.

## TABLE OF CONTENTS

ABSTRACT .....	iv
ACKNOWLEDGMENTS .....	vi
LIST OF FIGURES .....	viii
INTRODUCTION .....	1
MATERIALS AND METHODS.....	7
RESULTS .....	14
DISCUSSION.....	46
REFERENCES .....	51

## LIST OF FIGURES

Fig. 1. Major pathway of apoptosis illustrated by <a href="http://www.apoptosisworld.com">www.apoptosisworld.com</a> .....	3
Fig. 2. Annexin positive cell .....	15
Fig. 3. AnnexinV stained cultures indicating no virus-enhanced apoptosis. ....	16
Fig. 4. Cycloheximide treated cells stained with DAPI. ....	17
Fig. 5. Determination of nuclear morphology as a marker for apoptosis in infected and uninfected cells .....	18
Fig. 6. Effect of staurosporine (5 $\mu$ M) on EBTr cells. ....	19
Fig. 7. Gel of the extracted DNA. ....	20
Fig. 8. Detection of caspase activated cells in virus-infected cultures and in control cells. ....	22
Fig. 9. Unsynchronized uninfected control cells for cell size .....	24
Fig. 10. Infected cells in the unsynchronized culture .....	26
Fig. 11. Unsynchronized control cell. ....	27
Fig. 12. Unsynchronized BPV infected cells. ....	28
Fig. 13. Synchronized control cells. ....	31
Fig. 14. Synchronized infected cells #1 .....	34
Fig. 15. Synchronized cells #2 .....	37
Fig. 16. Synchronized control cells. ....	38
Fig. 17. Synchronized BPV infected cells #1 .....	39
Fig. 18. Synchronized BPV infected cells #2 .....	40
Fig. 19. Infectivity assay. ....	42
Fig. 20. HA titers showing release of hemagglutinin into the media .....	43
Fig. 21. LDH activity assay. ....	44

## INTRODUCTION

Parvoviruses are small, nonenveloped icosahedral viruses with linear single stranded DNA genomes of about 5 kb in size. There are two open reading frames (ORFs) in the genomic DNA. The left ORF encodes nonstructural proteins required for viral DNA replication. The right ORF encodes the structural proteins of the virus. The mRNAs are capped and polyadenylated. The mammalian parvoviruses are divided into two genera on the basis of helper virus requirement (4). The genus Dependovirus, also referred to as helper-dependent viruses, consists of the defective viruses that require coinfection with adenovirus or herpesvirus. They are adeno-associated viruses (AAVs). The autonomous parvoviruses, also referred to as helper-independent viruses, which include bovine parvovirus (BPV), canine parvovirus (CPV), feline panleukopenia virus (FPV), H-1, LuIII and minute virus of mice (MVM), do not require a helper virus for productive infection. However, due to their low genetic complexity, autonomous parvoviruses are dependent on cellular factors that are expressed as a function of proliferation and differentiation in order to complete their life cycle. Although they require S phase for complete replication, they are incapable of inducing cells to enter mitosis, thus the infection remains cryptic until host cells enter S phase for DNA replication (14, 18).

BPV, an autonomous parvovirus, was isolated in 1961 from the gastrointestinal tracts of calves by Abinanti and Warfield (1). The virus was first known as HADEN (hemadsorbing-enteric) virus (1). It causes gastroenteritis and mild respiratory symptoms in cattle (32, 28, 21). Free virus attaches to sialic acid to mediate the hemagglutination reaction (33) and to bind to bovine cells in culture (15). The host range

of the virus is relatively narrow, primarily infecting cattle but low titered antibodies have been found in goats, dogs, and horses. High antibody titers have been found in cynomolgus monkeys and guinea pigs (31). It is pH stable, lipid solvent stable and heat stable (2, 25). The average diameter of the virus particle was revealed to be 20 nm by electron microscopic examination. The DNA genome contains two non-identical terminal palindromic sequences that have cis signals important in replication steps. The genome replication model includes a hairpin transfer mechanism (5, 3). Like the other autonomous parvoviruses, BPV DNA replication requires actively dividing cells. BPV does not contain a virion-associated DNA polymerase, thus cellular DNA polymerase is required for the synthesis of viral DNA. The genome encodes two nonstructural proteins and three structural proteins (13). The major structural polypeptide is VP3 and it accounts for 75%-83% of the virion protein. The molecular weight of VP3 is about 67,000. VP1 has a molecular weight of 85,500, while VP2 has a molecular weight of 77,000. Both VP2 and VP3 are minor capsid components. After protein synthesis, the viral proteins are translocated to the nucleus, where the assembly process is completed. Egress of the virus is presumably by degradation of the cell and rupture of the nuclear membrane (14).

There has been a great deal of research into the basic biology of parvoviruses. An area of significant interest in virus biology is the cytolytic effect of viruses in infected cells. Viruses can kill the infected cells by inducing apoptosis or necrosis or other types of cell death. Apoptosis is an active process of cell death that is tightly controlled. It is called “programmed cell death” because it is the purposeful removal of useless, unwanted, or damaged cells. It can be divided into two phases: the initiation phase and

the effector phase. The initiation phase involves caspases 8, 10 and 2, where these caspases are responsible for initiating apoptosis in the extrinsic pathway. The effector phase is common to all apoptotic processes where caspases 6, 7 and 3 are involved (16). Caspases are cysteine proteases that cleave their substrates after aspartic acid residues (10).

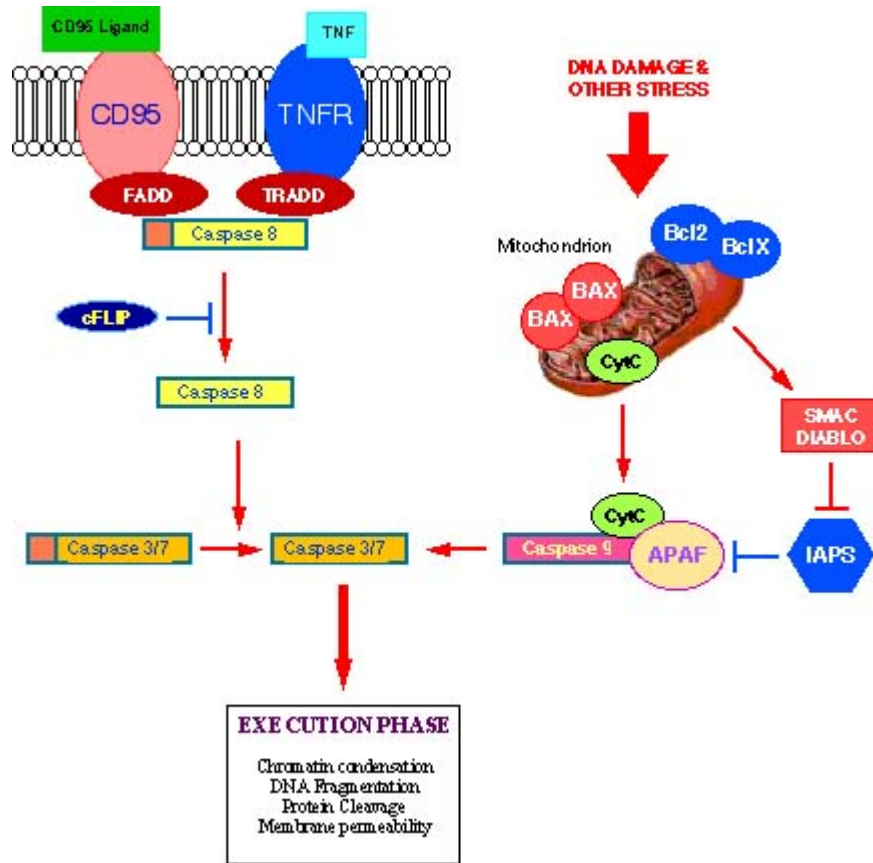


**Fig. 1. Major pathway of apoptosis illustrated by [www.apoptosisworld.com](http://www.apoptosisworld.com).**

Cells undergoing apoptosis show characteristic morphological and biochemical changes, such as the appearance of phosphatidylserine molecules on the outer surface of the plasma membrane. Another feature is the presence of a nucleosomal ladder due to

non-random DNA fragmentation by caspase-activated DNase and other DNase (10, 34).

Many virus genomes encode gene products that induce apoptosis which may contribute directly to their cytopathogenic effects (30). Two of the viruses that induce apoptosis are human immunodeficiency virus (HIV) and vesicular stomatitis virus (VSV).

HIV kills T cells by inducing apoptosis. Activated T cells produce Fas receptor, which is related to the TNF family and binds Fas ligand which is a membrane protein. The HIV proteins Nef, Tat and SU have a role in increasing the production of Fas ligand (FasL). When Fas on activated T cells binds to a FasL on HIV infected cells, the receptor trimerizes, triggering a signal transduction cascade that results in apoptosis of the activated T cell. In this case the extrinsic apoptotic pathway is involved. HIV induction of apoptosis in T cells contributes directly to the pathogenicity of the virus (29).

VSV induces apoptosis by activating the intrinsic pathway. The viral matrix protein induces apoptosis via the mitochondrial pathway due to the inhibition of host gene expression. This inhibition causes a stress in the cell that initiates the formation of the apoptosome. Apoptosome formation involves cytochrome release from the mitochondria, Apaf-1 and caspase 9 (8, 17, 20).

On the other hand, there are viruses that inhibit apoptosis of the infected cells by the action of viral anti-apoptosis proteins (16). These viruses inhibit apoptosis, prolonging the life of the cell, so that they can replicate and form progeny virions. An example of a virus that inhibits apoptosis is adenovirus. Adenovirus has several proteins that inhibit apoptosis. E1B 19kDa is a Bcl-2 homolog that inhibits the intrinsic pathway. E1B 55kDa inactivates p53 by binding directly to p53 and blocking its ability to activate transcription. p53 is a transcription activator and a tumor suppressor (30). Moreover, E3

10.4/14.5 kDa internalizes Fas (which is the receptor), thus inhibiting the extrinsic pathway.

Studies on how viruses induce cell death in the target cells have been done on several members of the Parvoviridae family. Parvovirus H-1 was studied to assess whether it is able to kill human hepatocellular carcinoma cell line QGY-7703. Data from this study support that H-1 virus kills QGY-7703 cells, which are permissive cells, by a nonapoptotic process (19, 27). However, parvovirus H-1 was reported to induce apoptosis in non-permissive cells such as C6 rat glioblastoma cells, Hep3B and HepG2. H-1 induces apoptosis in C6 rat glioblastoma cells by a caspase-3-dependent apoptosis activation pathway (26). The significance of this study was the possibility of considering parvoviruses as vectors for tumor-cell gene therapy because the virus is oncotropic and oncolytic gene therapy seems possible (23). Additionally, studies have been done on B19 of the genus erythrovirus (the only known human parvovirus pathogen). B19 is the causative agent of erythema infectiosum (fifth disease). The nonstructural protein (NS1) was found to be responsible for inducing apoptosis in erythroid lineage cells by a pathway that involves caspase 3 activation (24, 6). Moreover, B19 NS1 protein induces apoptosis in nonpermissive cells such as HepG2 by directly damaging cellular DNA leading to mitochondrial stress and activation of caspase 9 and caspase 3. Further, feline panleukopenia virus was shown to induce apoptosis in feline lymphoid cells (12). This viral induced cytotoxicity might relate directly to viral pathophysiology of atrophy of lymphoid tissues associated with feline panleukopenia (12).

Necrosis, another form of cell death, involves a different way of cell killing. Necrosis is called “accidental” cell death, contrasting it from programmed death. It is the

process which occurs when cells are exposed to serious physical or chemical insult. Typical changes that occur in necrosis include cytologic swelling, mitochondrial changes, and plasma membrane breakdown (cytolysis). The burst releasing the content of the cytoplasm to the environment triggers, if occurring *in vivo*, a damaging inflammatory response. The DNA is fragmented in a random fashion that appears as smears on electrophoresis gels without the appearance of the DNA fragment laddering characteristic of apoptosis. Moreover, no caspase involvement has been shown in necrosis. Some viruses kill the target cells by inducing necrotic cell death. The infected host cell might also trigger necrosis so the released cytoplasmic content of the cell in the intercellular space would promote an inflammatory response, thus activating phagocytes and attracting leukocytes into the necrosis zone. It is suggested that under pathophysiological conditions, necrotic cell destruction should amplify and catalyze the pathological processes .

Reportedly, bovine parvovirus has a cytolytic effect on infected cells (7). So far there are no data on how BPV kills the infected cells and whether cytolysis is a direct effect of virus activity, or an indirect effect of cell response to viral infection. Thus, this study was undertaken to add information to the understanding of BPV biology. In this project, we studied whether BPV induces apoptotic cell death, or induces necrotic cell death. Various approaches were used to identify the type of induced cell death. Data collected from the different approaches do not support the suggestion that BPV kills infected cells by inducing apoptosis, rather the data support the notion that virus kills the host cell by a pathway leading to necrotic cell death.

## MATERIALS AND METHODS

**Virus, cells and media.** The virus used in this study was the original BPV isolate obtained from F.R. Abinanti, NIH. It was passaged in primary bovine embryonic kidney cells, then in bovine tracheal cells. The embryonic bovine tracheal cells (EBTr), a diploid cell strain, were originally obtained from the American Type Culture Collection (ATCC, Rockville, MD). The media used in this study were Dulbecco Modified Eagle's Medium (DMEM) containing 0.11% sodium bicarbonate, 10 mM HEPES buffer, 50 µg/ml of gentamycin and either 5% cosmic calf serum (HyClone, Logan, UT) or Fetal Clone III serum product (HyClone). Cosmic calf serum contains anti-BPV antibody, therefore, in cultures where virus infection was measured, the media contained Fetal Clone III and not cosmic calf serum.

**Annexin-V-FITC apoptosis staining.** EBTr cells were cultured on round coverslips (12mm) in shell vials in 5% fetal clone III DMEM. Various sets of shell vial cultures were prepared for annexin staining to show phosphatidylserine inversion in apoptotic cells. The sets included BPV infected cells, positive controls and negative controls. The positive controls used consisted of cells exposed to cycloheximide (1000 µg/ml) incubated at 37°C for 24 h. The second positive control set used consisted of cells exposed to staurosporine (5 µM) which was added to the cells and incubated at 37°C for 4 h. In the virus-infected cell set, BPV was added to cells at a multiplicity of infection (MOI) of 0.27 and incubated at 37°C for 48 h (two replication cycles) to ensure that most of the cells were infected. Negative controls consisted of uninfected and untreated EBTr cells grown in 5% Fetal Clone III DMEM. The stain reagents were obtained as a kit from

BioVision (Mountainview, CA) and the instructions in the package insert were followed with minor technical adjustments. Unfixed cells were stained by adding annexin-V-FITC reaction mixture (10 $\mu$ l of annexin-V-FITC and 5 $\mu$ l of propidium iodide) and incubated at room temperature for 10 min in the dark. The cells were then washed with phosphate buffered saline (PBS) and distilled water and placed on microscope slides and inspected microscopically under UV illumination for apoptotic positive cells. Apoptotic positive cells that had bound Annexin-V-FITC showed green staining in the plasma membrane, while negative cells remained unstained.

**4',6-diamidino-2-phenylindole (DAPI) staining.** EBTr cells were cultured on coverslips in shell vials in 5% Fetal Clone III DMEM. Various sets of shell vials were prepared for DAPI staining including BPV infected cells, positive controls and negative controls. Staurosporine at a concentration of 5  $\mu$ M was used as the positive control and was incubated with cells at 37°C for 4 h. BPV was added to cells and incubated at 37°C for 48 h, as described above for annexin-V staining. Negative controls were EBTr cells with no virus or other treatment. Then the cells were placed on microscope slides that had drops of mounting fluid that contained DAPI stain. The DAPI stain consisted of phosphate buffered glycerin (pH 9) containing 0.02 g per 100 ml p-phenylenediamine and 0.05 mg per 100 ml of DAPI. Cells were analyzed under fluorescence microscopy for nuclear morphology changes. Apoptotic positive cells were morphologically defined by nuclear shrinkage and chromatin fragmentation.

**DNA Fragmentation as an indicator of apoptosis.** Four 75 cm<sup>2</sup> flasks of cultured EBTr cells at 70% confluency were prepared. One culture was used as a negative control, another culture served as a positive control where staurosporine (5  $\mu$ M)

was added to the cells and incubated at 37°C for 6 h. Dimethyl sulfoxide (DMSO) was added to the third culture as an additional negative control, while the culture in the fourth flask was BPV infected (MOI=0.0066). The cultures were incubated until complete cytopathic effect (CPE) was achieved. Then the cells were trypsinized and collected for DNA extraction. Cells were washed by centrifugation with PBS three times, then the pellets were treated with 100 µl of lysis buffer (1% Triton x-100 in 20 mM EDTA, 50 mM Tris-HCl, pH 7.5) for 10 sec. After centrifugation for 5 min at 1600 x g, the supernates were collected and the extraction was repeated by using the same amount of lysis buffer. The supernates were brought to 1% sodium dodecyl sulfate (SDS) and then treated by RNase A (final concentration 5 µg/µl) for 2 h at 56°C. Then digestion was carried out with proteinase K (final concentration 2.5µg/µl) for 2 h at 56°C followed by the addition of ½ volume 10M ammonium acetate. The DNA was then precipitated with 2.5 volumes of cold (-20°C) 100% ethanol and left overnight at -20°C. The samples were then centrifuged at 325 x g for 25 min and resuspended in 70% ethanol (300 µl per pellet). After suspending the pellets, the samples were centrifuged at 325 x g for 10 min and left to air dry for 30 min. The pellets were resuspended in 50 µl of TE (1mM EDTA and 10 mM Tris-HCl) overnight at 8°C. The DNA was electrophored in 1.5% agarose gel at 100 volts for 3-4 h until the tracking dye ran in a distance of two thirds of the gel. Gels were then stained with SYBR green for 20 min. Apoptotic cells would show a ladder DNA on agarose gels (11).

**CaspGLOW fluorescein caspases staining.** EBTr cell cultures on coverslips in shell vials were grown in 5% fetal clone III DMEM and the various sets of infected and control cells were as described above for annexin-V staining. The principle of the kit was

the addition of an FITC labeled caspase inhibitor VAD-FMK. VAD-FMK binds irreversibly to many activated caspases such as caspase 1, 3, 4, 5, 6, 7, 8, 9. The CaspGlow reagent kit was obtained from BioVision and the directions on the package insert were followed with minor technical adjustments. Following preparation of the culture sets, the cells were stained by adding FITC-VAD-FMK reaction mixture (1  $\mu$ l of FITC-VAD-FMK in 300  $\mu$ l of wash buffer) to each coverslip and were incubated for 1 h at 37°C in an atmosphere containing 5% CO<sub>2</sub>. Then the cells were placed on microscope slides and were analyzed by fluorescence microscopy. Caspase positive cells showed bright green staining, while negative cells remained unstained.

**Cellular morphology of non-synchronized cells.** Experiments were performed to assess morphological changes in infected cells compared to uninfected cells. Cell swelling was assessed as a marker for cell death by necrosis. EBTr cells were cultured in 25 cm<sup>2</sup> flasks. Two flasks were prepared. One flask was a control that contained cells in 5% fetal clone III. The second flask contained BPV infected cells (MOI = 2.85) in 5% fetal clone III DMEM. These cultures were incubated at 37°C for 34 h. Pictures of the cells were taken at 10, 12, 14, 16, 18, 20 and 34 h post-infection. Then the cells were stained with immunoperoxidase (IP) stain for virus antigen-positive cells by the method previously described (15, 22) and as detailed below. The surface areas of cells were measured 5 times by using a computer program (Spot advanced) and the means and standard deviations were calculated.

**Cellular morphology of synchronized cells.** EBTr cells were cultured in 25 cm<sup>2</sup> flasks with the desired concentration of synchronizing medium (DMEM, 5% fetal clone III and 2 mM hydroxyurea) and incubated for 32 h. Then the cell cycle block was

released by washing the cultures in serumless medium for three times and then the media were renewed with 5% fetal clone III DMEM. Then the cells were infected with BPV (MOI= 2.85) while another culture was a control. Pictures of cells were taken every 2 h post-infection (2, 4, 6, 8, 10, 12, 14, 16, 18, 20, 22, 24, 26, 28, 30, 32). The cells were stained with IP stain for virus antigen positive cells. The surface area of cells were measured 5 times by using the computer program and the means and standard deviations were calculated.

**Infectivity assays.** Experiments were carried out to determine the release of cell cytoplasmic contents as an indicator of cytolysis by the necrotic pathway. The markers assessed were infectious cell-released virus, viral hemagglutinin, and the cell enzyme lactate dehydrogenase. In these experiments, EBTr cells were grown in monolayers to 90% confluency and then the cells were washed with serumless media and renewed with 5% fetal clone III DMEM. BPV was inoculated in one culture at an MOI of 0.006 and another culture served as negative uninfected control. The cultures were incubated at 37°C until complete (4+) CPE was achieved. During this incubation period 1ml samples from the media were taken every 6 h and centrifuged in a microfuge, to remove any unattached cells collected in the samples and the supernates were collected. Infectivity assays on the supernates were performed in flat sided tissue culture tubes (Nunc) to detect infectious virus particles that were released into the media of the cultures. For the assays, dilutions of the supernates were combined with media and cell suspensions and incubated at 37°C for 2 days in Nunc tubes. Following incubation, the cells, having formed monolayers were fixed with FAA fixative (formaldehyde, ethanol and acetic acid) and

stained with IP stain for virus antigen-positive cells. Cells were visualized under light microscopy and positive cells were counted and infectious virus titers determined.

**Haemagglutination (HA) assays.** These assays were run in 96-well U-bottomed plates. Samples were diluted 1:10, 1:100 and 1:1000 in HA buffer (gelatin and bovine serum albumin, reference 4). 50 µl of each diluted sample were mixed with 50 µl of 0.5% human type O red blood cell suspension and the plate was incubated at 4°C overnight. Negative results were scored as red cell button formation, whereas positive results were scored as agglutinated, cell sheets. To obtain a final titer, two fold dilutions between the ten-fold steps were tested as needed.

**Lactate dehydrogenase (LDH) enzyme assays.** Supernates of media collected from infected and control cells in the experiments designed to test release of cell cytoplasmic contents were tested for LDH enzyme activity. The assay reagents were purchased in a kit from Roche Diagnostics Corp. (Indianapolis, IN). The manufacturer's procedure was followed. The assay was run in flat bottomed wells where 100µl of samples were added to 100 µl reaction mixture (250 µl of catalyst, Diaphorase/NAD<sup>+</sup> with 11.25ml of dye solution containing iodotetrazolium chloride and sodium lactate). The wells were incubated for 30 min at 15-25°C in the dark. Following the incubation period, the absorbances of samples were measured at a wavelength of 490 nm using an ELISA plate reader.

**Immunoperoxidase stain.** For IP staining to identify infected cells, the procedure previously described (4) was used. Briefly, guinea pig anti-BPV antibody was added to FAA fixed cells following washing and incubated at 37°C for 30 min with periodic agitation. After incubation, the cells were washed with distilled water and

peroxidase-enzyme conjugate was added, and the cells were incubated at 37°C for 30 min with periodic agitation. The cells were then washed, again with distilled water, and the chromagen (4-chloro-naphthol) was added, and the cells were incubated at 37°C for 30 min. Following incubation, the cells were washed and the cultures were inspected under light microscopy. Viral antigen-positive cells have black stained nuclei.

## RESULTS

**Assessment of infected cells for apoptosis by Annexin-V-FITC staining.** Cells undergoing apoptotic cell death *in vivo* must be distinguished by the immune system and cleared by macrophages without promoting an inflammatory response, a pattern that is completely different from necrotic cell death. In necrosis cells burst and release their contents, thus promoting an inflammatory response. Macrophages can recognize apoptotic cells by different ways. For example, macrophages can recognize altered sugar groups on the apoptotic cell surface. Macrophages also secrete thrombospondin which acts as a bridge between the macrophage and an apoptotic cell. Another way that macrophages recognize apoptotic cells is by recognizing phosphatidylserine, which is a negatively charged phospholipid that is normally confined to the cytosolic surface of the plasma membrane lipid bilayer, but relocates to the extracellular surface in apoptotic cells. The annexin-V-FITC reagent is used to detect phosphatidylserine on the extracellular surface. Annexin V is a protein that has a high affinity for phosphatidylserine and is used to detect phosphatidylserine molecules. Detection is analyzed by using fluorescence microscopy. Positive cells show green staining in the plasma membrane (see Fig. 2).

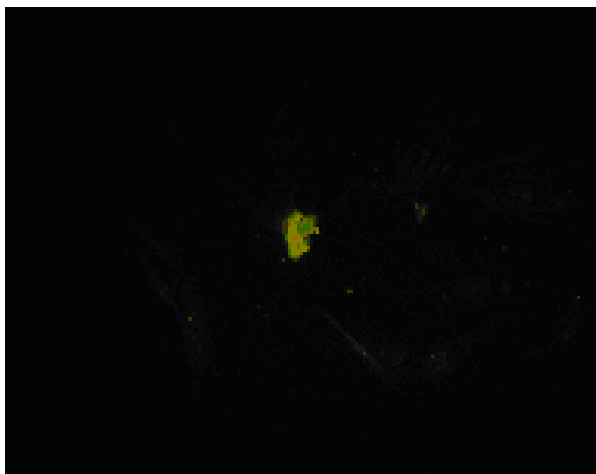


**Fig. 2. Annexin positive cell.** Apoptotic cells show green staining in the plasma membrane while unstained negative cells are in the background of the microscopic field.

Various cell sets were prepared to be stained by annexin-V-FITC stain. The first cell set was composed of five shell vials of control cells (negative control), the second was composed of five shell vials of cells incubated with staurosporine (positive control). The third set contained five shell vials of cells incubated with cycloheximide (positive control). The fourth set was composed of five shell vials of BPV infected cells. The cells in each of the culture sets were stained with Annexin-V-FITC stain for the detection of apoptotic positive cells. Another cell set of infected cells was prepared, and this set was stained with IP stain for virus antigen-positive cells.

The positive cells were counted in each shell vial by scanning through the entire coverslip for positive cells. The means and standard deviations in each of the five culture sets were determined and shown in Fig. 3.

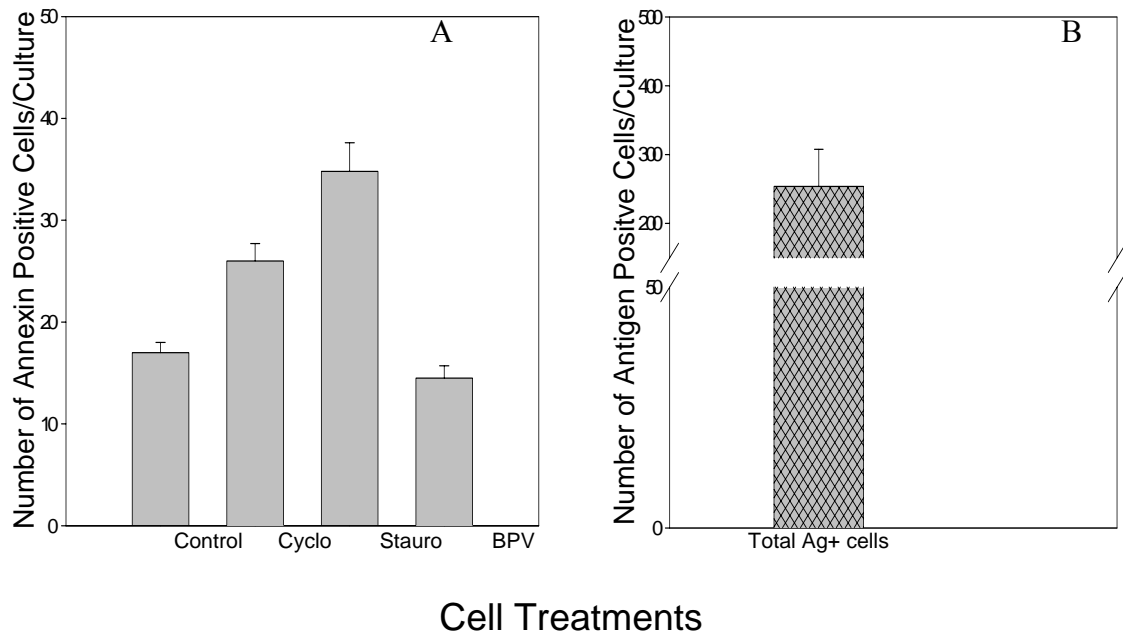


**Fig. 3. Annexin V stained cultures indicating no virus-enhanced apoptosis.** In A, each bar represents the number of annexin positive cells presented as the mean of 5 results. The bar in B, represents the number of virus antigen positive cells also represented as the mean of 5 results. The number of annexin positive cells in the infected cultures were indistinguishable from the negative control cultures.

The results shown in Fig. 3 indicate that, on average, the number of apoptotic positive cells in the two positive controls were higher than in the negative control or BPV infected cells. Therefore, the stain reagents worked properly but the virus did not induce positive cell formation that was different from the negative control. The number of virus positive cells is also higher than the number of apoptotic cells in BPV infected cells.

**Assessment of nuclear changes in infected cells.** Among the cardinal signs of cells undergoing apoptosis are chromatin condensation followed by DNA fragmentation with observable nuclear morphological changes. DAPI stain was used to detect these

nuclear morphological changes which are due to signals that induce an apoptotic cell death response. Stained nuclei were inspected under fluorescence microscopy. Apoptotic positive cells were morphologically defined by nuclear shrinkage and chromatin fragmentation. Shown in Fig. 4 is a photomicrograph of a culture induced with cycloheximide. In this culture about 1 in 138 cells showed nuclear evidence of apoptosis.

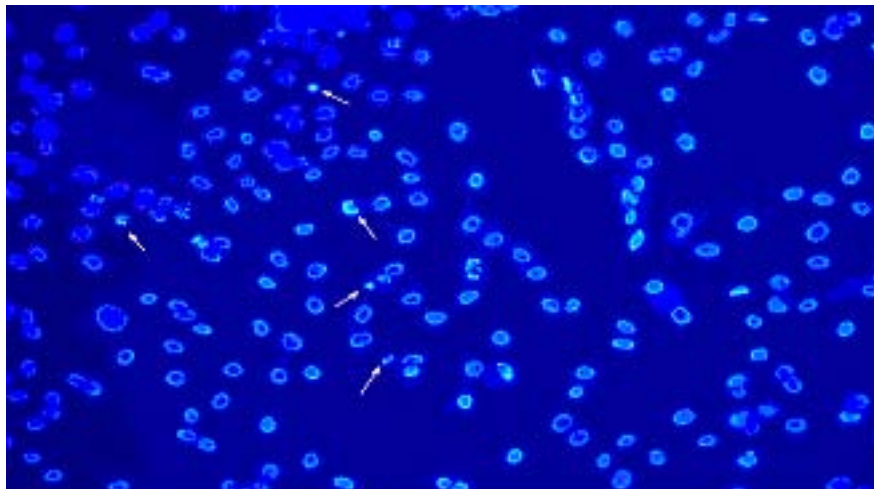


**Fig. 4. Cycloheximide treated cells stained with DAPI.**

Cells undergoing apoptosis show nuclear shrinkage and chromatin condensation (arrows), but most of these cells have morphologically intact nuclei.

Four cell sets were prepared to be stained by the DAPI stain. The first cell set was composed of five shell vials of control cells (negative control), the second was composed of five shell vials of cells incubated with staurosporine (positive control). The third set was composed of five shell vials of BPV infected cells. Each of the shell vial cultures was stained with DAPI stain for the detection of apoptotic positive cells. The

fourth cell set, also infected cells, was prepared and this set was stained with IP stain for virus antigen positive cells, to confirm the numbers of actually infected cells.

The apoptotic positive cells were counted in each culture by scanning through the entire coverslip for positive cells. The means and standard deviations for each of the four culture sets were calculated and shown in Fig. 5.

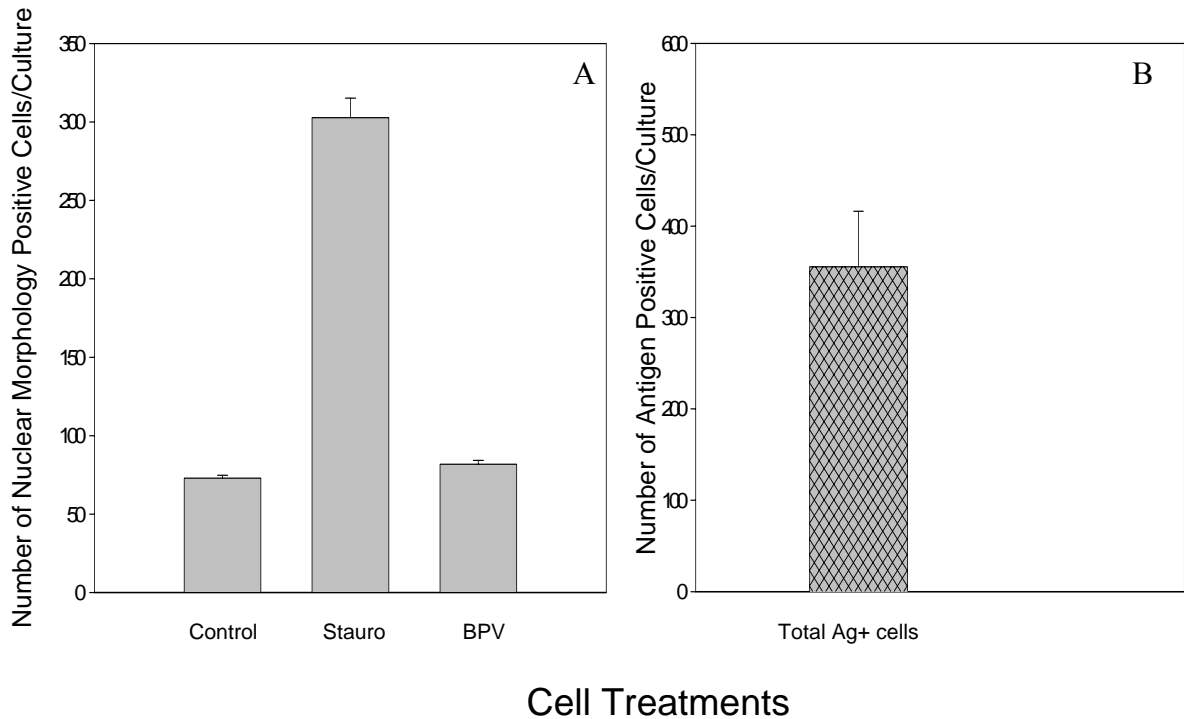


**Fig. 5. Determination of nuclear morphology as a marker for apoptosis in infected and uninfected cells.** Each bar represents the number of apoptotic cells presented as the mean of 5 results. The last bar represents the number of virus antigen positive cells also represented as the mean of 5 results. Equivalent numbers of apoptotic cells appeared in the infected cultures and the negative control culture.

The results indicated that, on average, the number of apoptotic positive cells in the positive control was higher than in the negative control or in the BPV infected cells. There was no significant difference between the infected cells and the negative control

cells. The number of virus positive cells was also higher than the number of apoptotic cells in any of the cultures, confirming a high level of infected cells. Fig. 6 shows a photomicrograph of staurosporine treated cells, which shows marked alterations of gross cellular anatomy which are characterized by shrinkage and the nuclear changes noted above.

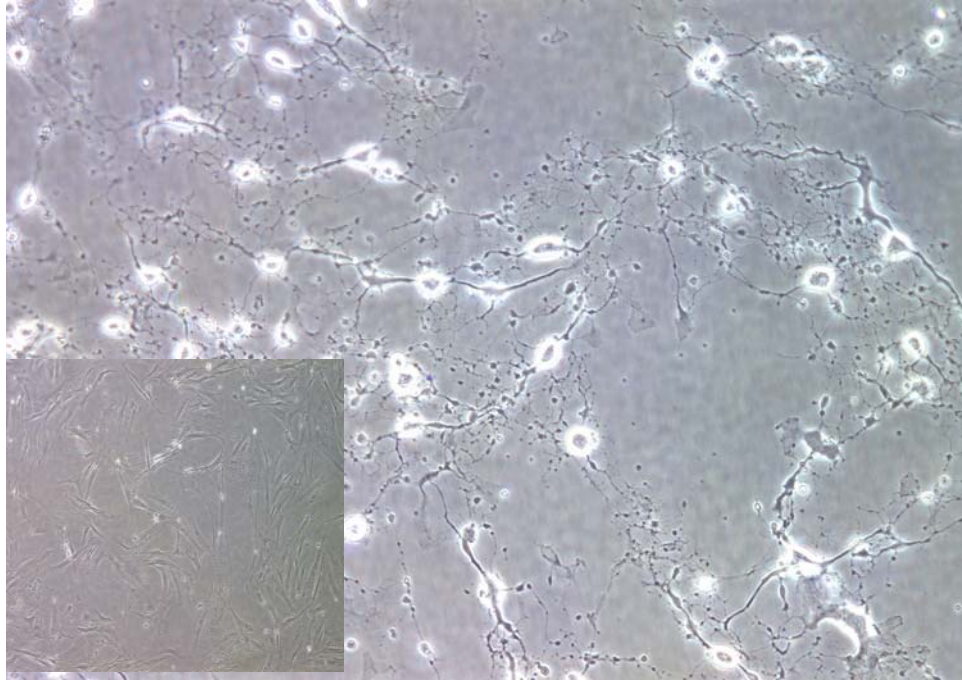


**Fig. 6. Effect of staurosporine (5  $\mu$ M) on EBTr cells.** Cells appear rounded and shrunken. The insert represents untreated EBTr cells.

**DNA fragmentation.** In positive apoptotic cells, the DNA fragments are separated in a non random fashion that yields DNA pieces that are multimers of about 180 bp of nucleosomal units that appear as DNA ladders on 1.5 % agarose electrophoretic gels. However, in necrosis, DNA is fragmented in a random fashion that looks like a smear on electrophoretic gels. The DNA of different cell treatments was extracted and electrophoresis of the extracted DNA was applied.

Fig. 7 represents a picture of the gel.

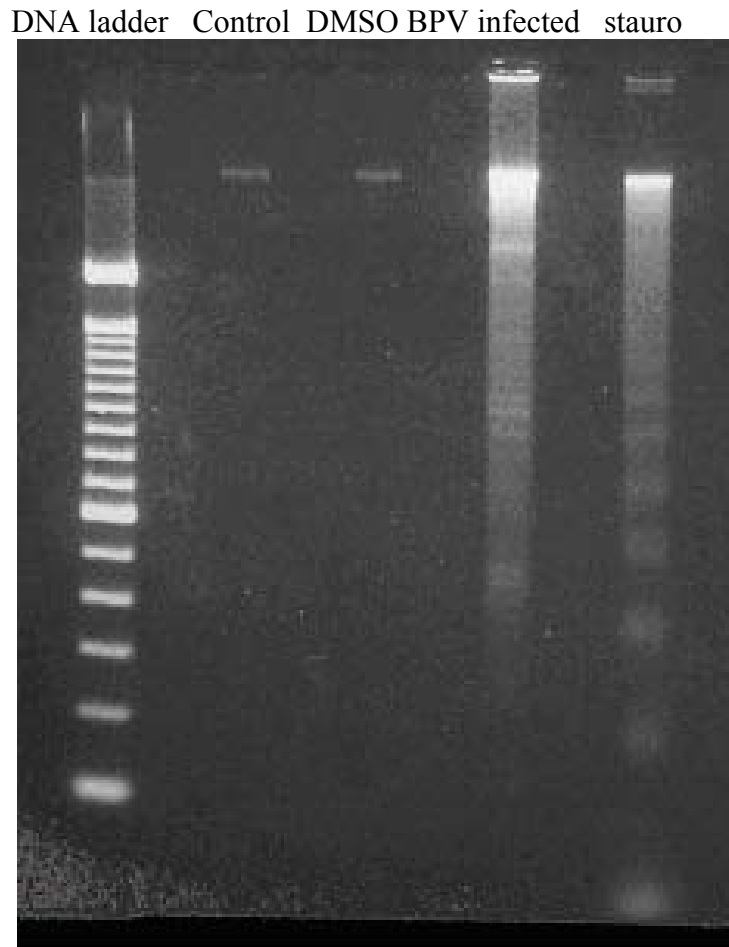


**Fig. 7. Gel of the extracted DNA.** The DNA bands in the control and DMSO treated cells are intact, while there is a DNA ladder in the staurosporine treated cells. The DNA in the BPV infected cells appears fragmented in a random fashion.

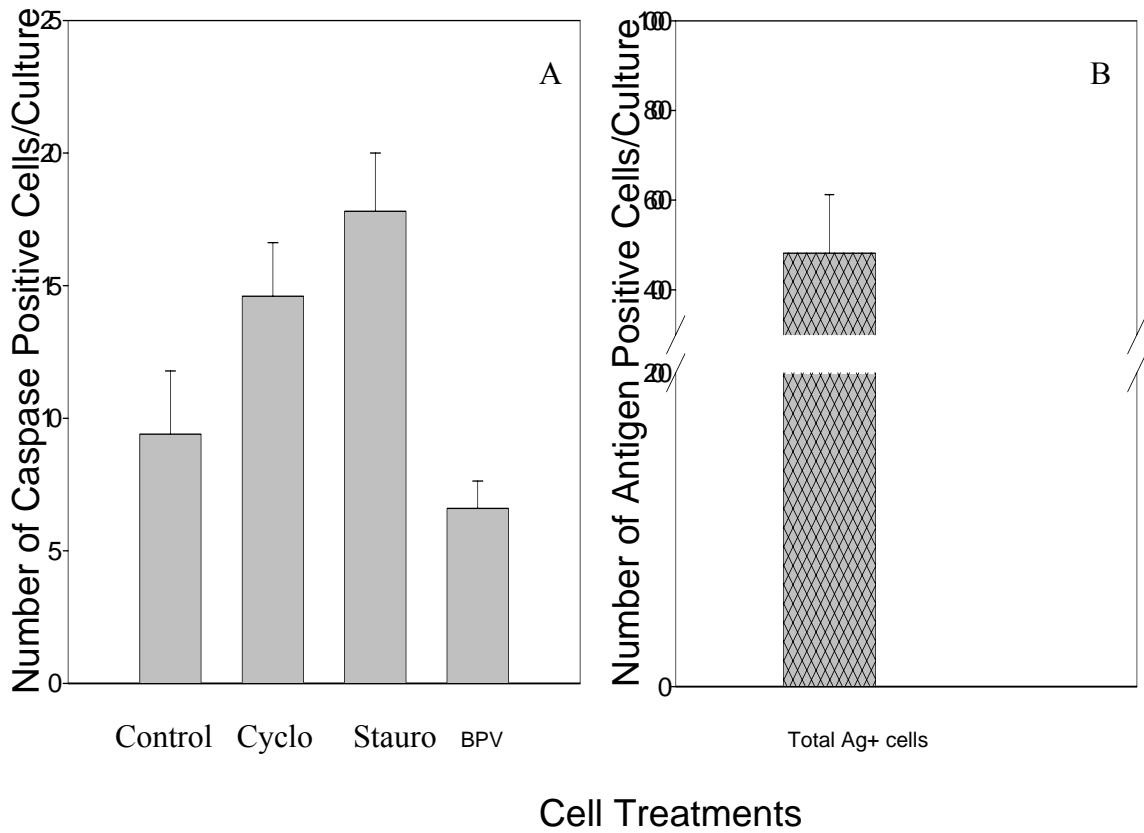
The gel separation of the DNA isolated from infected cells and positive and negative control cells is shown in Fig. 7. Both the negative control cells and DMSO treated cells had an intact DNA band. Cells treated with staurosporine (positive control) showed a DNA ladder of DNA fragments that are multimers. In BPV infected cells, the

DNA is fragmented in a random fashion forming a smear with no evidence of laddering. Presence of viral DNA is also suspected.

**Staining for caspases.** Caspases are proteases that are present in zymogen forms. These zymogens are composed of three domains; an N-terminal prodomain, p20 domain and p10 domain. In apoptotic cells, caspases are cleaved, thus they become present in their active form. The active form is a heterotetramer containing two p20/p10 heterodimers and two active sites. Caspases are subdivided into subfamilies based on their substrate preference and structural and sequence similarity (11).

This assay is a pan caspase assay. FITC-VAD-FMK molecules are used to bind and detect caspases. Detection is analyzed by using fluorescence microscopy. Positive cells show light green staining in the plasma membrane. Various cell sets were prepared for staining by the caspase stain. The first cell set was composed of five shell vials of control cells (negative control), the second was composed of five shell vials of cells incubated with staurosporine (positive control). The third set contained five shell vials of cells incubated with cycloheximide (positive control). The last set was composed of five shell vials of BPV infected cells. Each of the cultures was stained with caspase stain for the detection of apoptotic positive cells. Another cell set was prepared, and this set was stained with immunoperoxidase stain for virus antigen positive cells to confirm the level of virus infection.

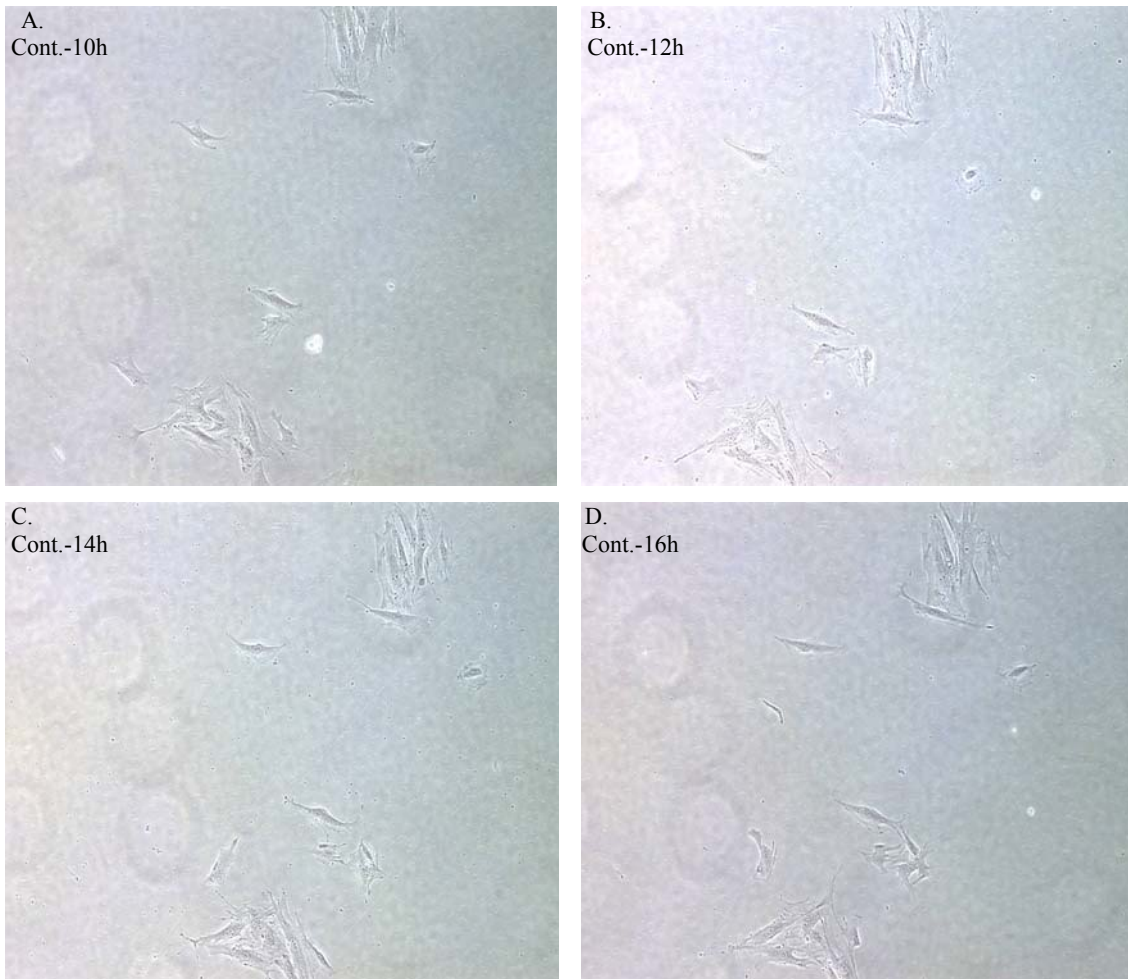
The positive staining cells were counted in each shell vial by scanning through the entire coverslip for positive cells. The means and standard deviations in each of the five shell vials of cell sets were calculated and shown in Fig. 8.

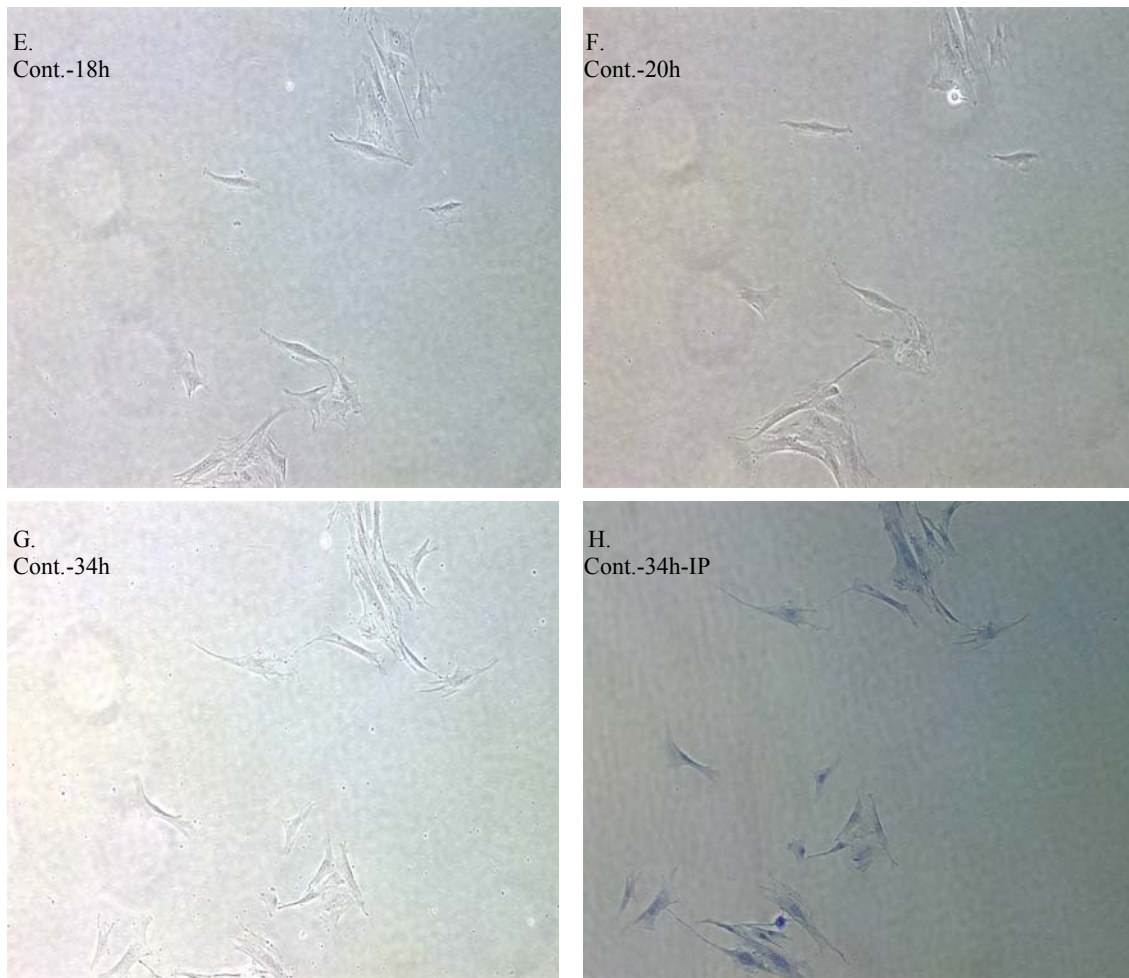


**Fig. 8. Detection of caspase activated cells in virus-infected cultures and in control cells.** In A each bar represents the number of apoptotic cells presented as the mean of 5 results. The bar in B, represents the number of virus antigen positive cells also represented as the mean of 5 results.

The results shown in Fig. 8 indicate that, on average, the number of apoptotic positive cells in the two positive controls were higher than in the negative control or BPV infected cells. The number of virus positive cells was also much higher than the number of apoptotic cells in the virus infected cells.

**Cellular morphology of non-synchronized cells.** Cells undergoing necrosis increase in size due to swelling, then they burst releasing their contents. Apoptotic cells undergo condensation of the chromatin and degradation of the DNA but do not swell. They shed tiny membrane-bound apoptotic bodies containing intact organelles which are then recognized and phagocytized by macrophages. In this assay cellular changes in morphology due to BPV infection were inspected and compared with cellular morphology of uninfected cells. The surface areas of cells were also measured to determine cell swelling. Comparisons of cell size between control cells and BPV infected cells were done. Pictures from the control cells taken at different time intervals are presented in Fig. 9.

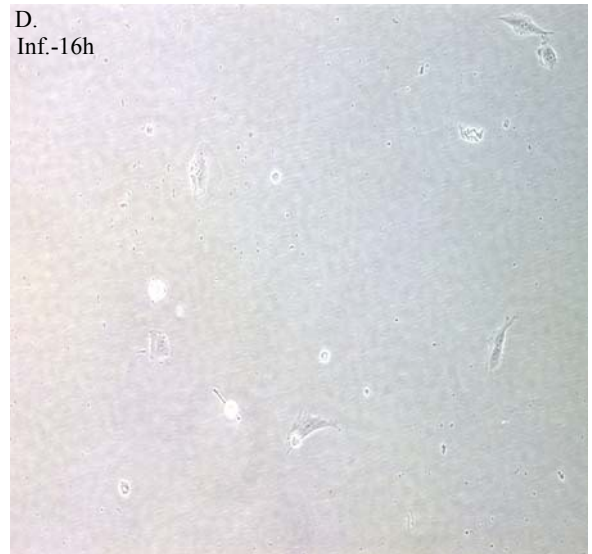




**Fig. 9. Unsynchronized uninfected control cells for cell size comparisons.** IP staining confirmed the cells were not infected.

The same microscopic field was followed through the course of the study. From following individual cells in the micrographs, it was deduced that control cells undergo cell division and show variation in the cell size through the incubation period, with a trend of size increase at the end.

Pictures from the infected cells taken at various time intervals are presented in Fig. 10.



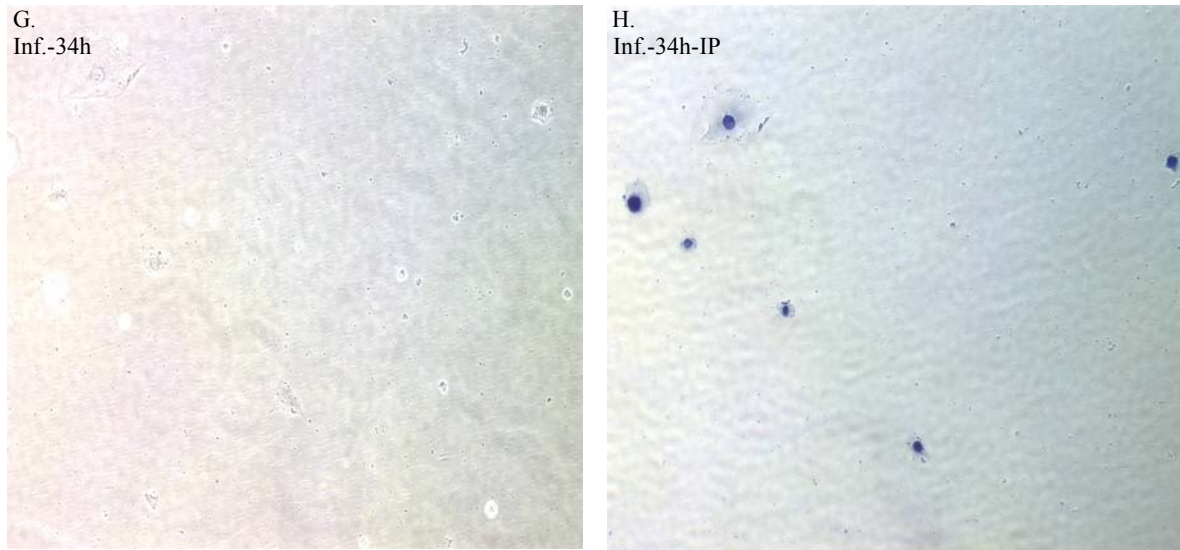


**Fig. 10. Infected cells in the unsynchronized culture.** A major feature of the infected cells was cell shrinkage then detachment following cytolysis. Panel H shows the same field as Panels A-G after IP staining.

From the pictures, it was deduced that the infected cells did not undergo cell division and the cells tended to increase in size followed by shrinkage and cell detachment. Fig. 10H represents BPV infected cells after 34 h post exposure that are stained to show antigen-positive cells. The results showed that all of the cells were infected. Three infected shrunken cells are seen in a line angling downward, left to right.

The surface area for each cell was measured and the means and standard deviations were calculated. The results for control cells and BPV infected cells were plotted as curves. Figs. 11 and 12 represent the data for control cells and BPV infected cells respectively.

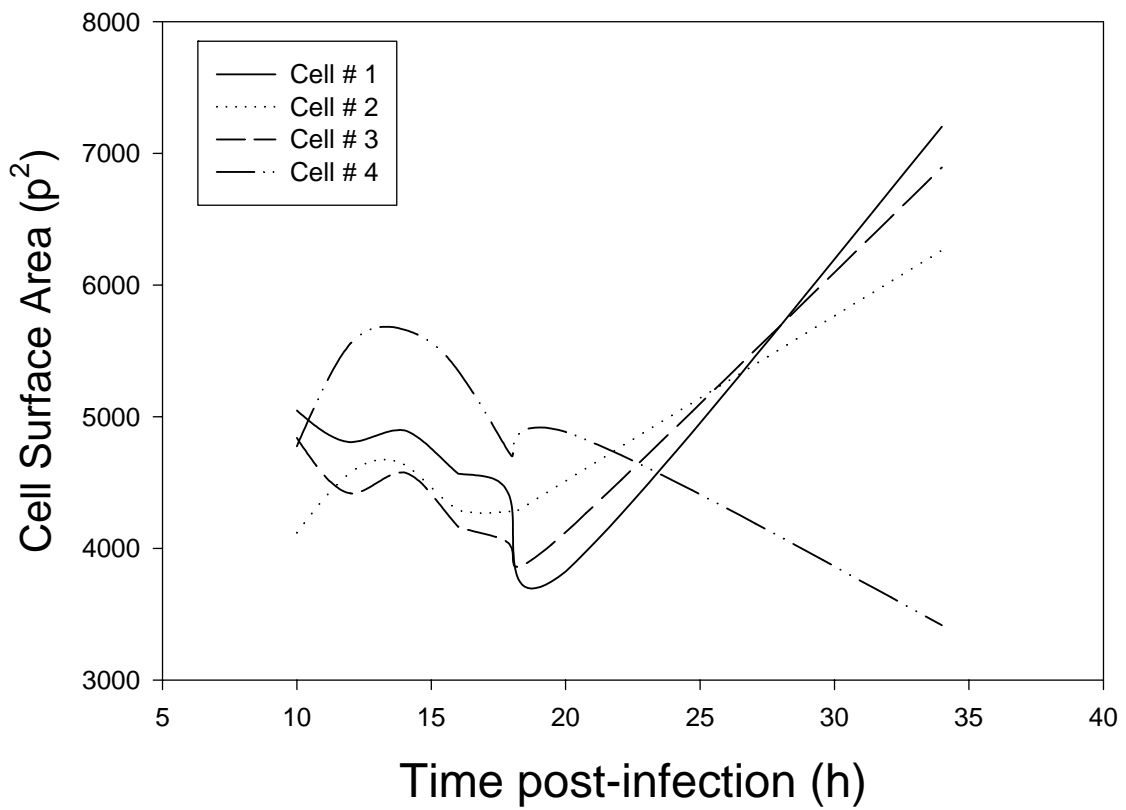


**Fig. 11. Unsynchronized control cell.** Surface areas in square pixels (p<sup>2</sup>). Over time none of the cells showed evidence of cytolysis nor detachment but there was size variation.

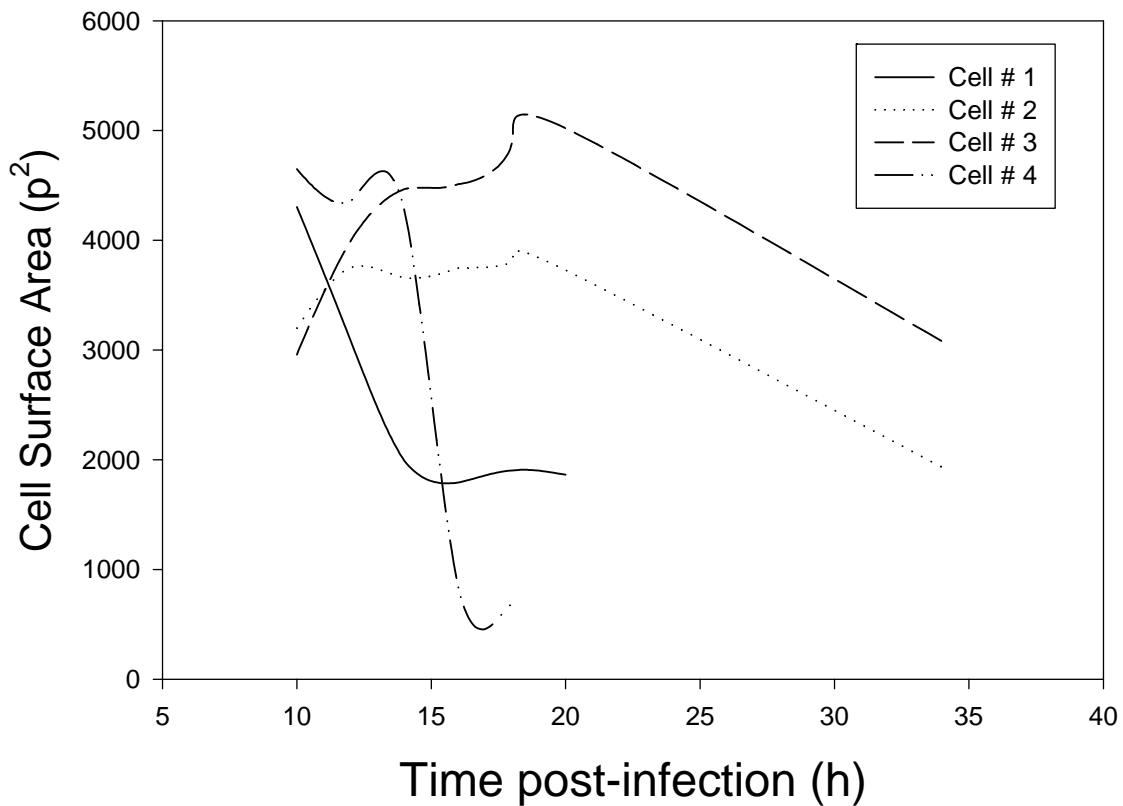
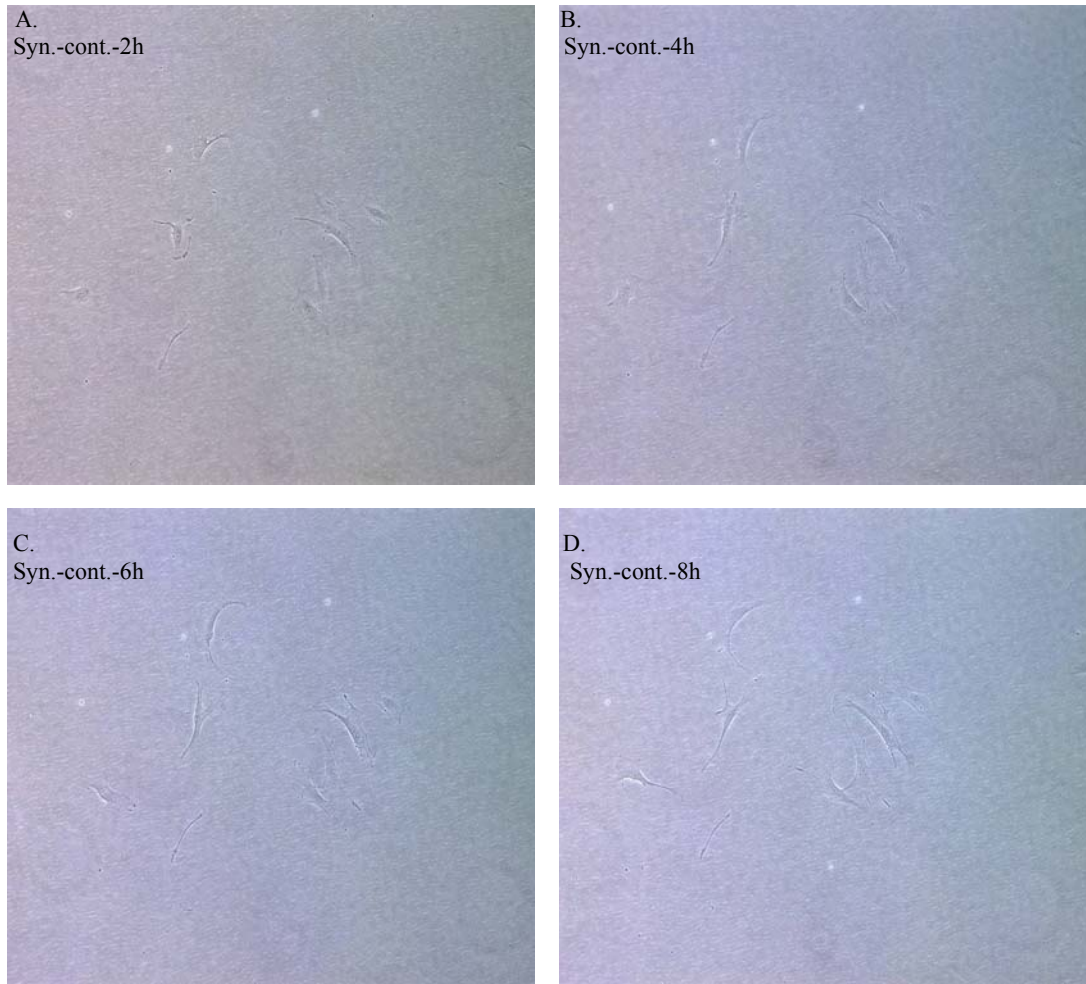


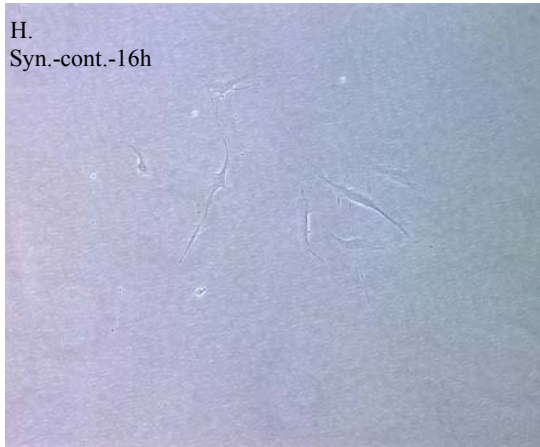
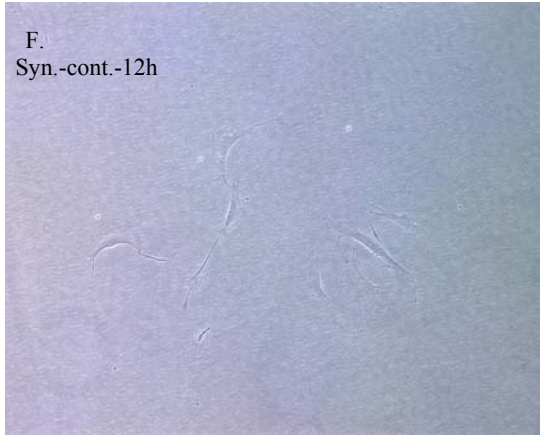
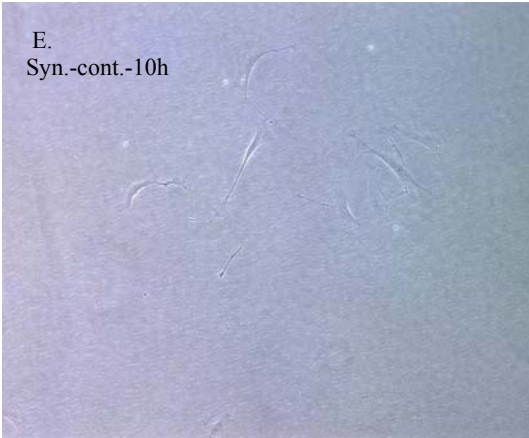
**Fig. 12. Unynchronized BPV infected cells.** The surface areas are expressed as square pixels ( $p^2$ ). All four of these cells shrank and detached, two very early, and two later in the course of infection.

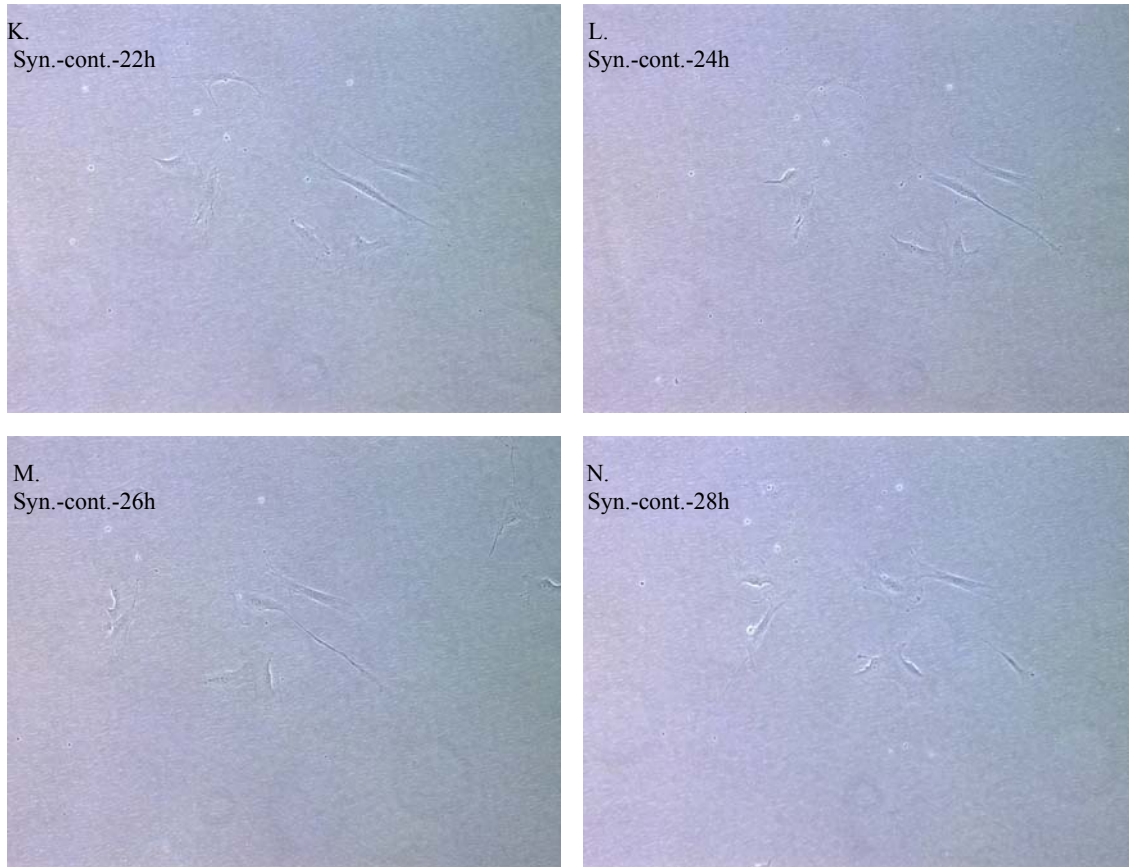
The pattern is different between these two populations of cells. The curves of the control cells show variance in size and an increase at the end consistent with preparation for cell division. However, the pattern in infected cells indicates that cells increase somewhat in size followed by marked shrinkage, then detachment indicating cell death.

**Cellular morphology of synchronized cells.** In this series of experiments cellular morphology changes due to BPV infection were inspected and compared with cellular morphology of uninfected cells. The cells used in this study were synchronized in the attempt to move cells through the cell death process in phase. Hydroxyurea was

used to block the cells in S phase. Release of the block, then infection should decrease the randomness seen in unsynchronized cultures. The surface area of cells was also measured and comparisons of cell size between control cells and BPV infected cells were done. Pictures of the control cells taken at various time intervals are presented in Fig. 13. The same microscopic field was followed throughout.



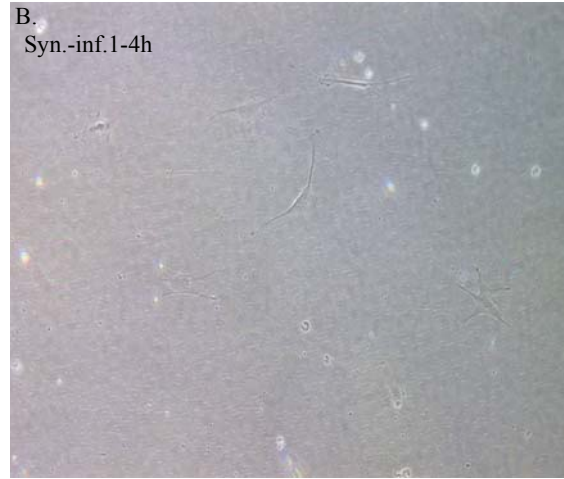
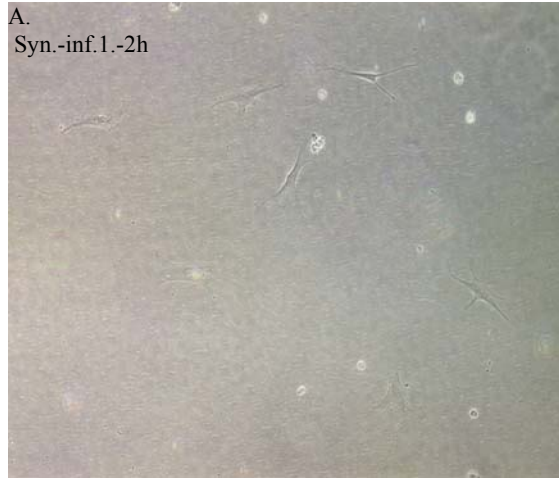


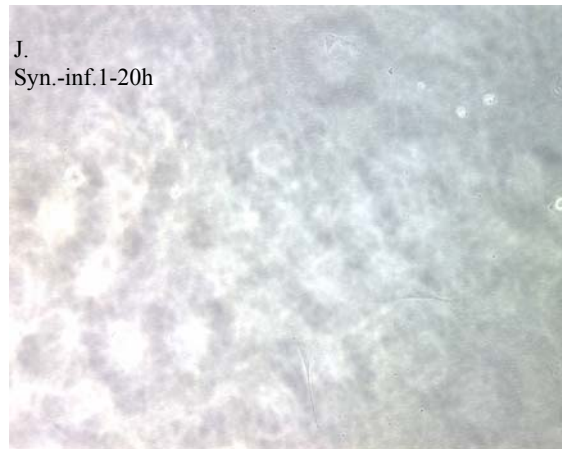
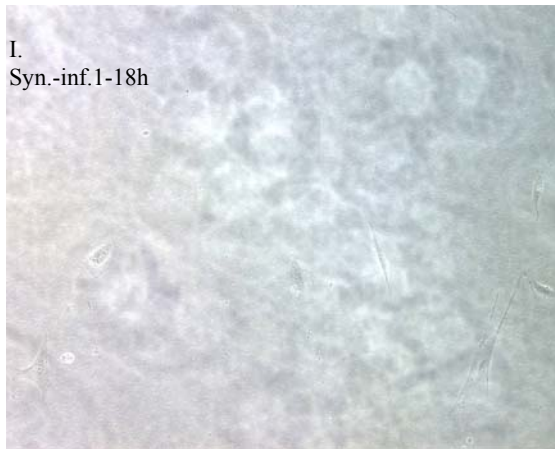
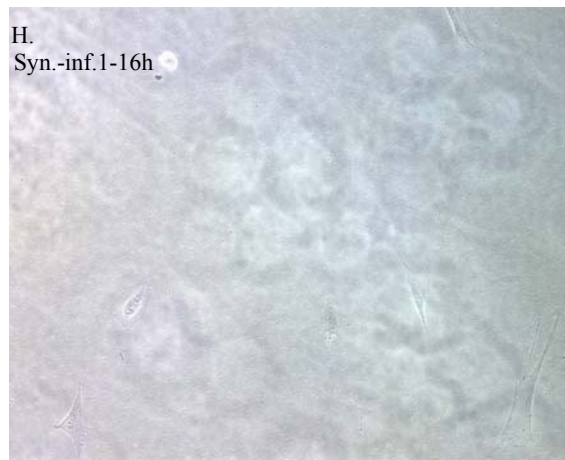
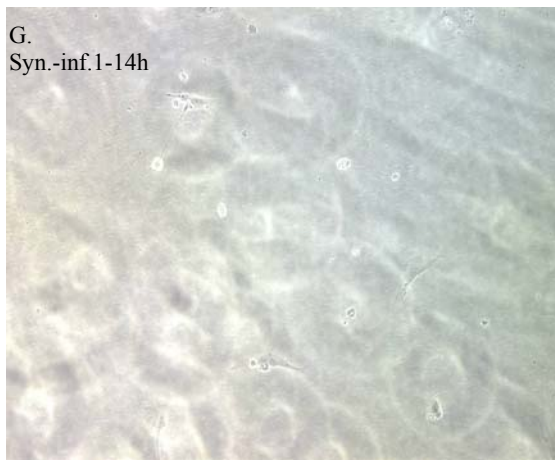
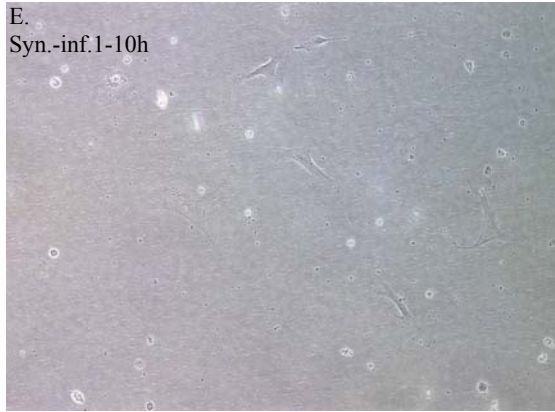


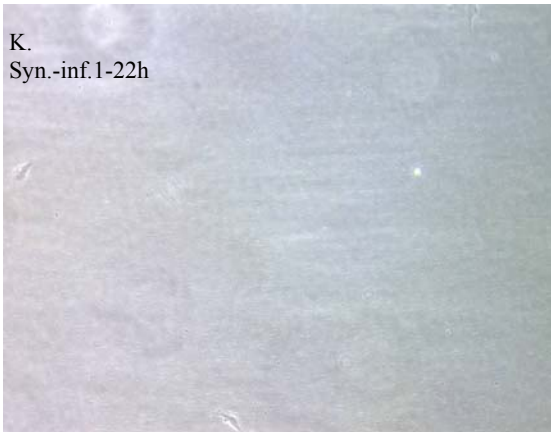
**Fig. 13. Synchronized control cells.** The cells vary with size as time varies with a trend of increase in size at the end. No cell shrinkage or detachment was detected.

From the pictures, it was deduced that control cells undergo cell division and show variation in the cell size through the incubation period, with a trend of surface area increase at the end.

To assess the cytological changes in synchronized virus-infected cells, two flasks of infected cells were prepared. One was kept until most of the cells were detached. While in the second flask, the cells were stained with IP stain before they detached, to confirm that the studied cells were BPV infected. Photomicrographs from the infected cells taken at different time intervals are presented in the following figure (Fig. 14). The first set of cells represents the cells that were left until detached.



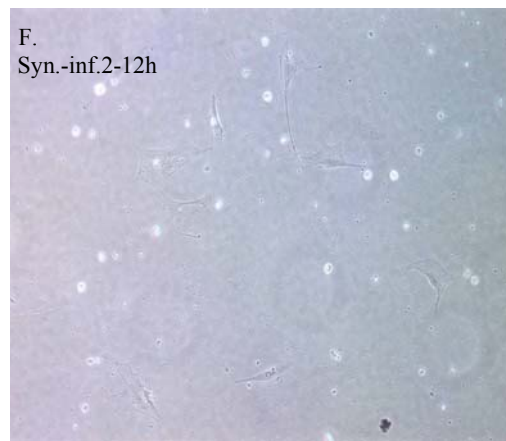
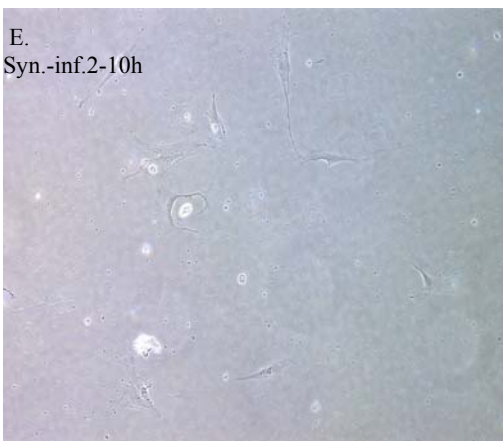
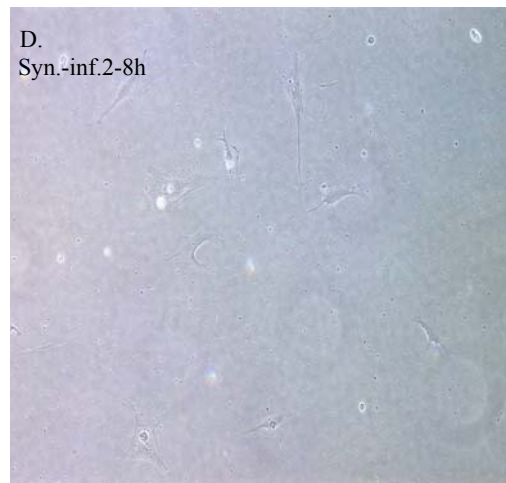
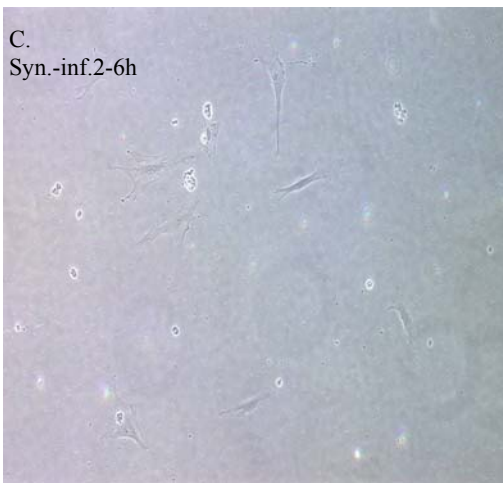
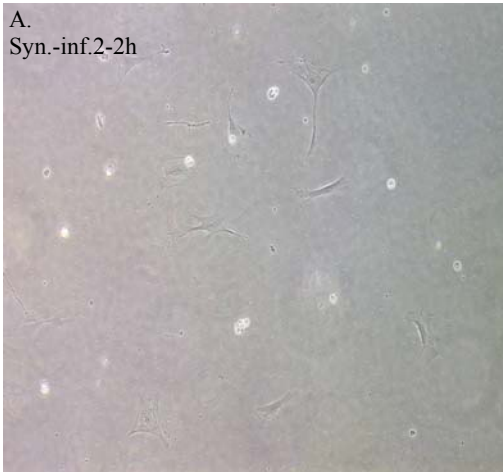


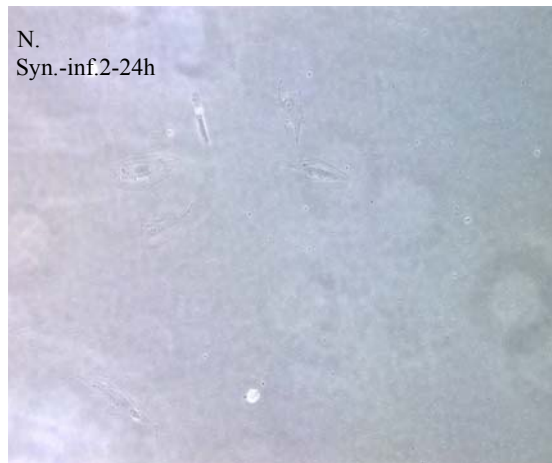
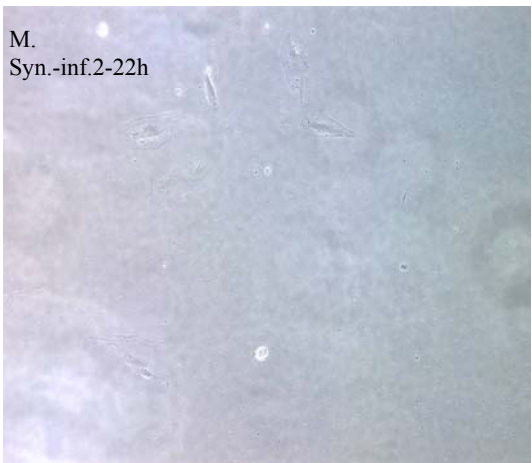
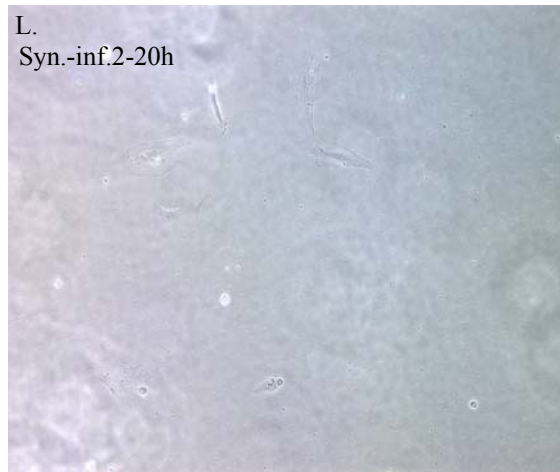
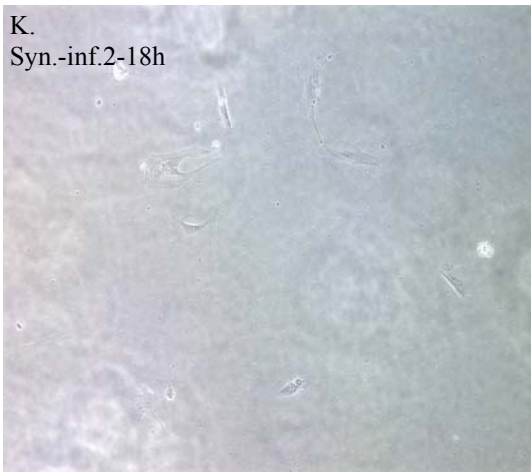
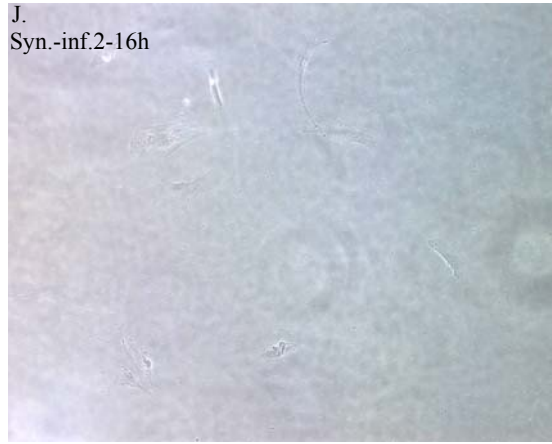
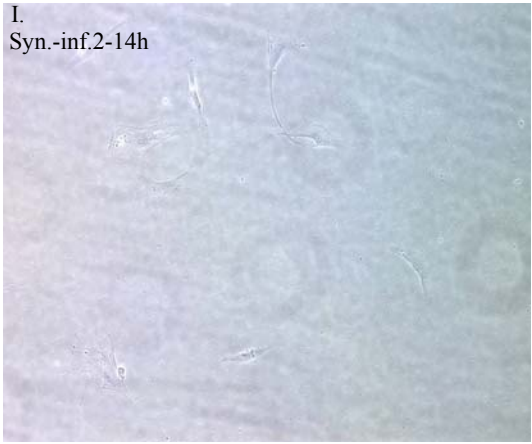


**Fig. 14. Synchronized infected cells #1.** Cells were seen to shrink and detach.

The pictures of infected cells imply that the cells increased somewhat in size before detaching. There were no cells dividing in the infected cells. Formation of apoptotic bodies is not seen in the dying cells.

The second cell set were the cells that were stained before detaching and stained with IP stain. The following figure (Fig. 15) represents the pictures taken for infected cells # 2.





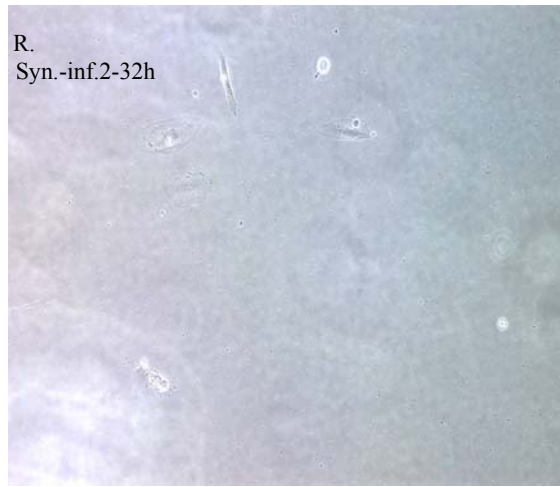
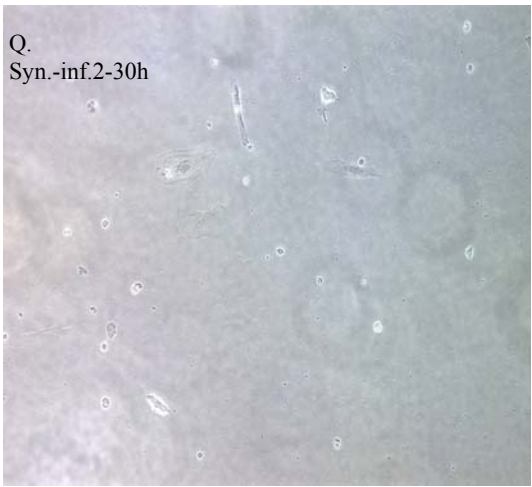
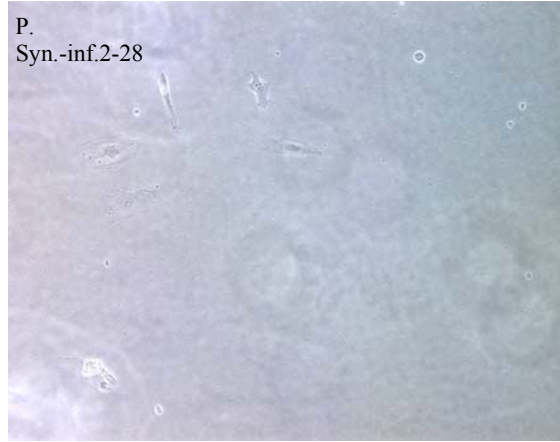


**Fig. 15. Synchronized cells #2.** The pattern detected with this cell set is cellular shrinkage followed by detachment.

From the pictures of infected cells, cell division does not occur, rather, the infected cells increased in size, then decreased. No apoptotic bodies were detected.

The surface area of each cell is plotted on curves, one for control cells (Fig. 16), the other is for infected cells #1 (Fig. 17) and the last one is for infected cells #2 (Fig.18). The pattern of the different cell sets were compared after looking at the curve plots. Fig. 16 illustrates the changes seen in the control cells: size variations with an overall trend toward growth over the 25 h test period.

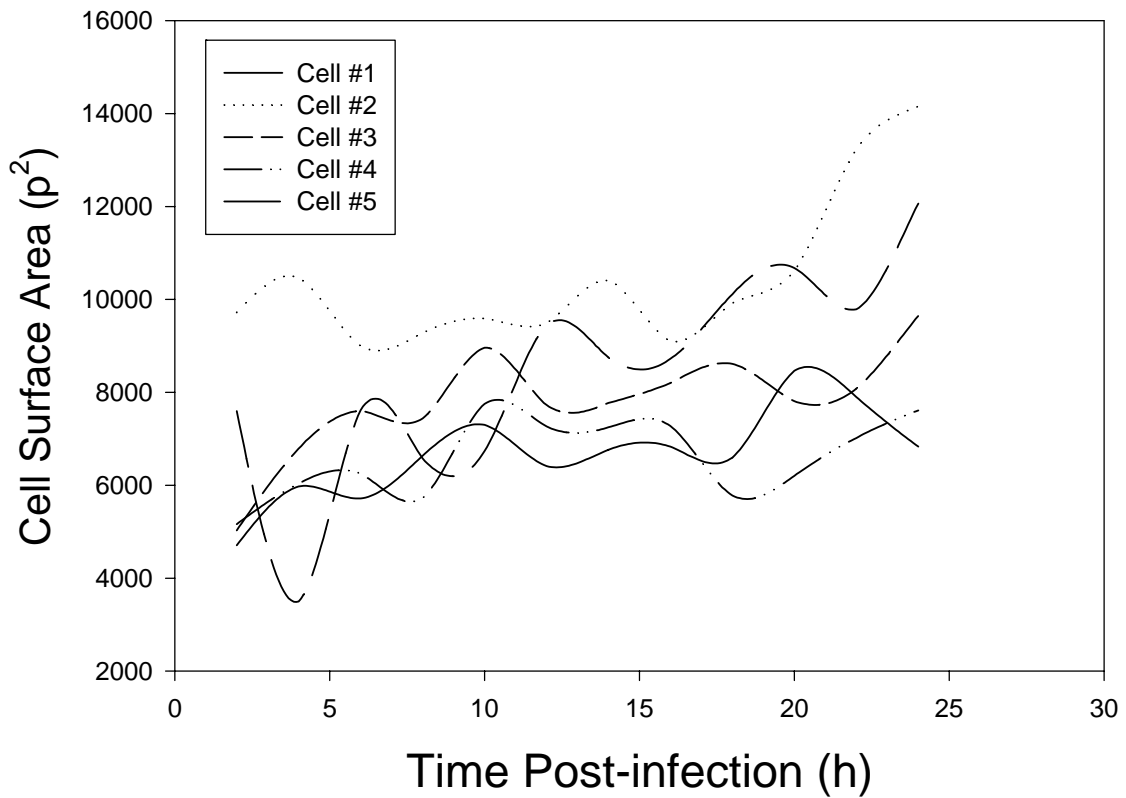


**Fig. 16. Synchronized control cells.**

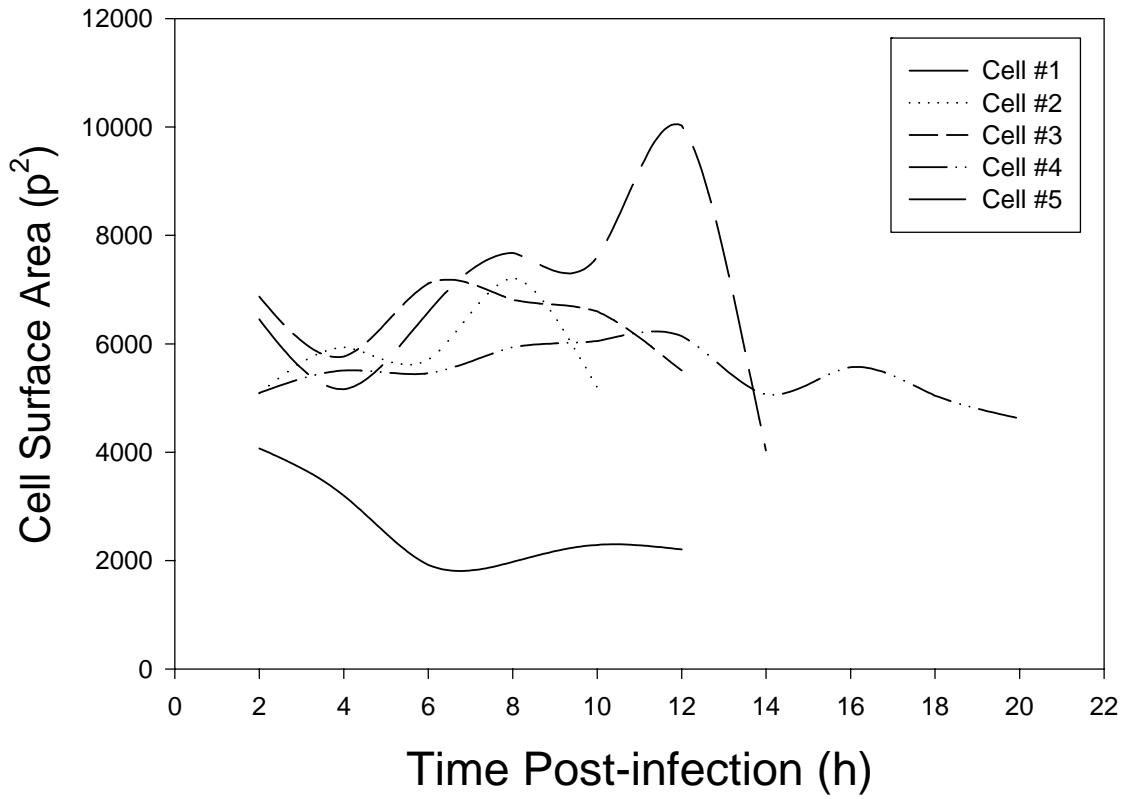


**Fig. 17. Synchronized BPV infected cells #1.** The surface areas are expressed square pixels (p<sup>2</sup>). Cells showed an increase in size, followed by shrinkage and detachment.

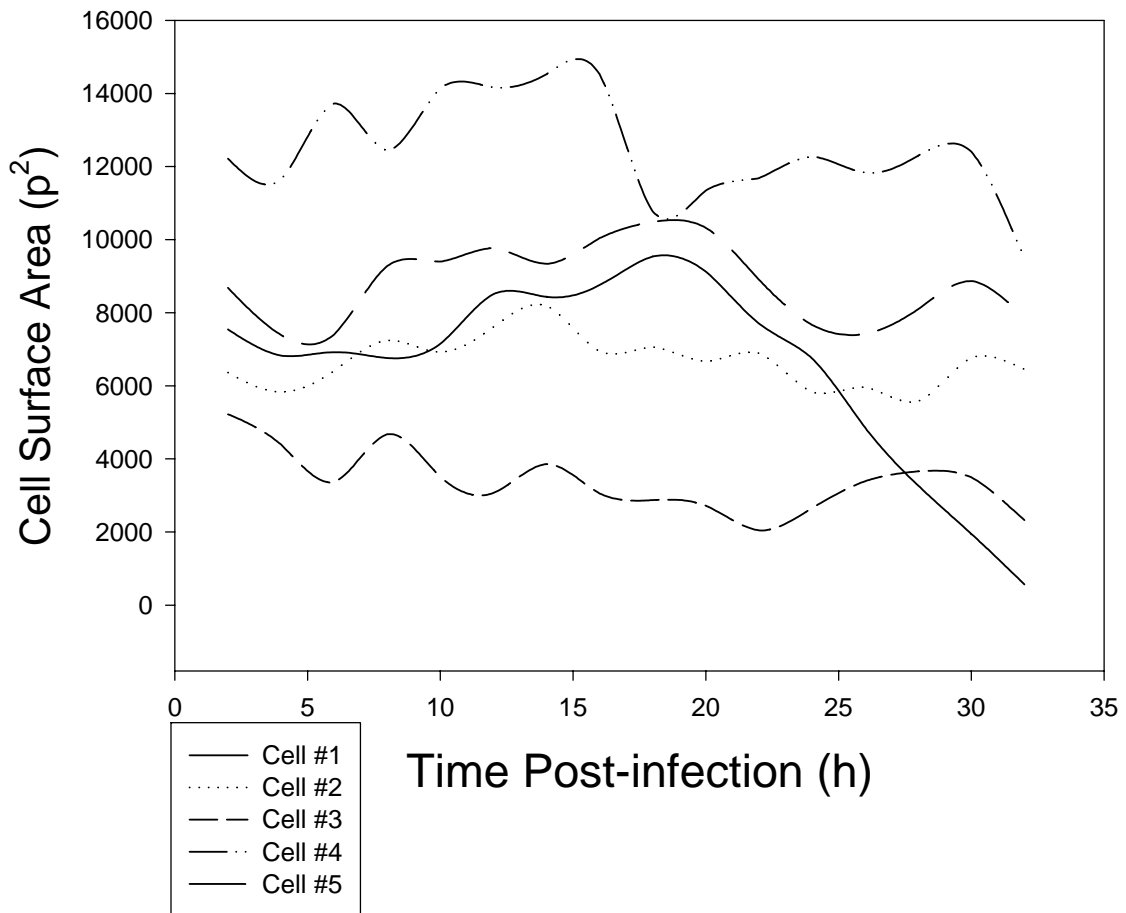


**Fig. 18. Synchronized BPV infected cells #2.** The surface areas are expressed square pixels ( $p^2$ ). The pattern deduced from this figure was that infected cells increase in size, which is then followed by shrinkage.

From the plots one can deduce that the control cells show a different pattern from the infected cells. The control cells, as noted, show a variation in the surface area, from increasing to decreasing to increasing and so forth until at the end most of the cells increased in size. However, the infected cells tended to decrease in size in the beginning then increase in size followed by shrinking and detachment.

Determination of cell death by necrosis in virus-infected cells by detecting the release of cytoplasmic and nuclear products. If BPV infected cells are killed by necrotic cell death, then it would be expected that the infected cells would burst releasing their contents into the media. Among the contents that might be dumped in the media are virus infectious particles. Since infectious virus is assembled in the nuclei, the release of intact viruses would indicate the failure of both the cytoplasmic and nuclear membranes. Infectivity assays were used to assess cell-released infectious virus particles in the media of cultured cells. Two cultures were prepared: one that was a negative control and the other was BPV infected. Media samples were collected at various time intervals and the last sample taken was when viral complete CPE was achieved at 104 h post infection. Also, at 104 h the remainder of the culture was freeze-thawed to disrupt the cells and release the cell-associated virus and hemagglutination. Assays of this sample should reveal the maximum available amounts of viral materials including virions. This sample is referred to as 104-m for maximum available titer at 104 h post-infection. Fig. 19 shows the results of infectious virus titrations detecting the number of virus infectious particles in the media supernates.

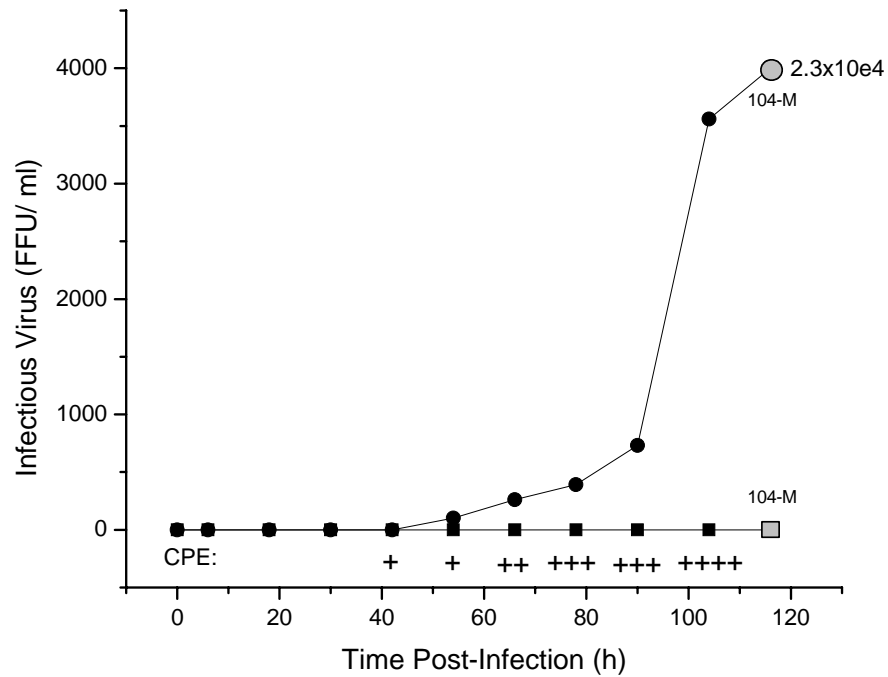


**Fig. 19. Infectivity assay.** Each line represents a different cell set. One represents the control (squares), while the other represents the BPV infected cells (circles). 104-m represents the maximum titer in the freeze-thawed sample at 104 h. CPE values are also recorded.

In the media collected from the negative control, no infectious particles were detected, while in the BPV infected culture, the number of virus infectious particles increased as CPE increased.

The release of soluble viral HA antigen together with particulate hemagglutinin was detected using HA assays. Cells undergoing apoptosis form apoptotic bodies, so no cytoplasmic contents are dumped in the surrounding environment. If infected cells die by necrosis then it is expected to find virus proteins in the media. This assay detects the titer of cell-released HA protein which is consistent with necrotic death. Two cultures were

prepared, one that was a negative control and the other was BPV infected. These were the same cultures that were assessed for infectious virus release. Samples from the media were taken at different time intervals. Fig. 20 shows the release of viral hemagglutinin during the course of infection.

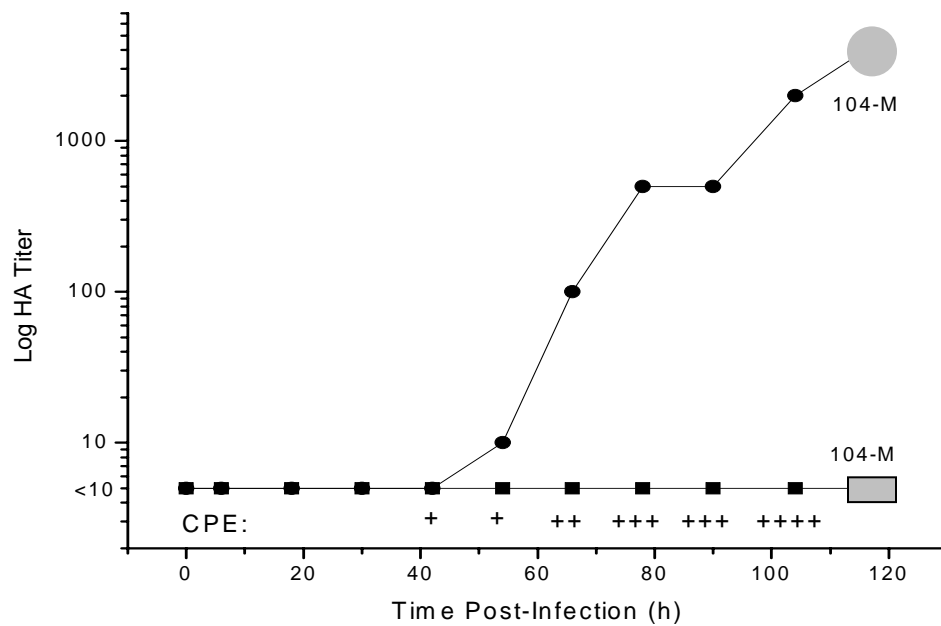


**Fig. 20. HA titers showing release of hemagglutinin into the media.** The squares represent the results of the negative control and the circles represent the results of the BPV infected culture. 104-m represents the maximum titer in the freeze-thawed sample at 104 h. CPE values are also recorded.

From the figure one can deduce that as CPE increased, the titer of HA protein increased in the supernates of the BPV infected culture. The control did not show any HA titer.

An additional approach for the detection of cytolysis is the determination of release of lactate dehydrogenase (LDH). Measurement of cytoplasmic enzyme activity released by damaged cells is an indicator of cytolysis. The amount of enzyme activity detected in the culture media is correlated to the proportion of lysed cells. In this assay LDH was used to assess cellular viability. LDH is a stable cytoplasmic enzyme present in all cells. Upon damage to the plasma membrane, LDH is rapidly released into the cell culture media. For this assay the same two cultures were used as were tested for infectious virus and hemagglutinin. Samples from the media were collected at various time intervals and centrifuged to remove contaminating cells. LDH activity was determined on the sample supernates and the results are reported in Fig. 21.

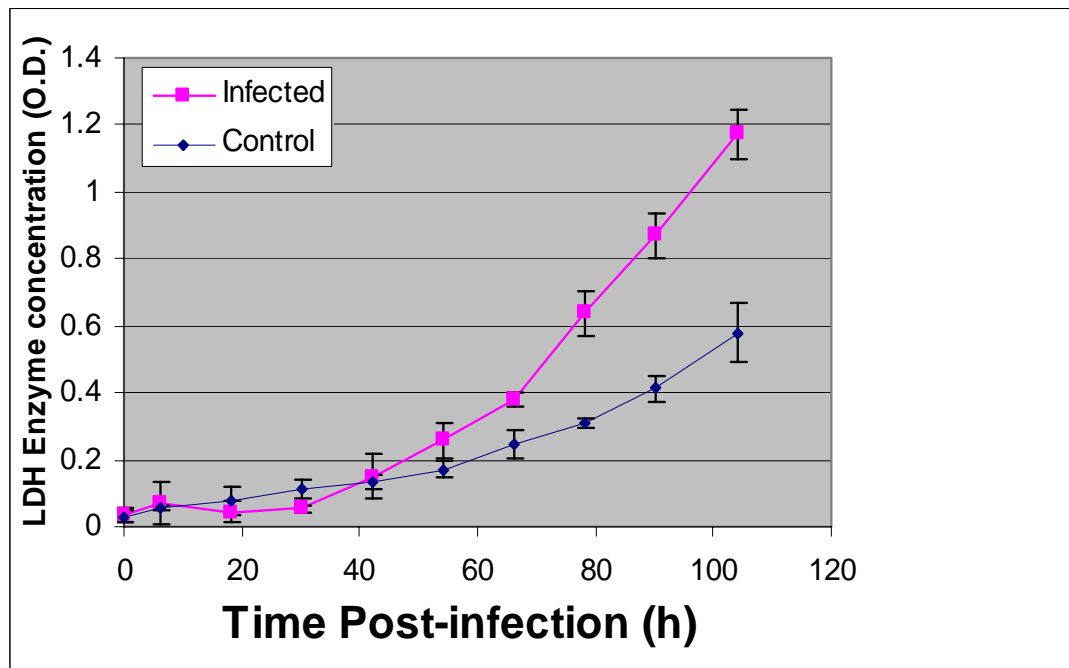


**Fig. 21. LDH activity assay.** One curve represents the control cells while the other represents the BPV infected cells. The figure indicates that LDH concentration increases with time, however, the increase is much higher in infected cells than in the control cells.

LDH concentration in both cultures is almost the same at the beginning of the experiment. As time post-infection increases, viral CPE was detected in the BPV infected cells. Also, after 42 h post infection, the concentration of the enzyme increased. Significantly higher levels of LDH were detected in BPV infected cell supernates than in the control cell supernates indicating necrotic cell damage in the infected cells.

## DISCUSSION

The final process in virus replication cycles is escape or egress from the infected cell. Different viruses solve this problem in different ways. Enveloped viruses bud through cell membranes: herpesviruses through the nuclear membrane and coronaviruses into Golgi for example. These viruses then escape the cell through the secretory pathway. Paramyxoviruses and orthomyxoviruses bud through the plasma membrane at the cell surface and the egress event is concomitant with maturation. The non-enveloped viruses that mature in the nucleus, such as adenoviruses and parvoviruses such as BPV, depend on physical disruption or programmed breakdown of the cell which can be triggered in a number of ways such as necrosis, apoptosis, or autophagy. Many viruses kill their host cells contributing directly to the virus-caused pathology seen in the infected person or animal. Some viruses kill the host cell by inducing an apoptotic cell death, usually by activating the intrinsic pathway of apoptosis. However, other cytolytic viruses tend to kill their host cell by inducing necrotic cell death. As mentioned in the introduction, some parvoviruses kill the infected cells by apoptosis while others use a non-apoptotic cell death pathway in killing infected cells. BPV is a cytolytic virus that causes acute gastroenteritis in calves. The pathways that BPV uses in killing the infected cells were not previously known, therefore this research was undertaken to study how BPV, as another model parvovirus, kills infected cells, and to investigate its mechanism of egress.

Cells undergoing apoptosis exhibit cardinal features such as non-random DNA fragmentation, phosphatidylserine exposure to the outer surface of the plasma membrane, and formation of apoptotic bodies. In this research several of these signs were looked for

in order to determine whether BPV infected cells undergo apoptosis. Annexin-V staining was used to assess phosphatidylserine translocation from the inner surface to the outer surface of the plasma membrane. This is used as an “eat me” flag for macrophages to recognize the apoptotic cell and clear damaged cells from the system without inducing an inflammatory response. Data from the Annexin-V staining experiment indicated that on average the number of apoptotic positive cells in the control and BPV infected cells were statistically indistinguishable. The numbers of apoptotic positive cells in the positive controls used were higher than those in the negative control cultures and in the BPV infected cells. If BPV induces apoptosis in infected cells, then the number of apoptotic cells measured by annexin-V staining is expected to be close to the number of antigen-positive BPV infected cells or at least similar to the positive controls. But that is not the case here; there was a significant difference between the number of viral antigen-positive cells and the number of apoptotic positive cells (Fig. 3).

Another approach to determine cell death by apoptosis is to observe cellular and nuclear morphology. The DAPI stain was used for this purpose. Cells undergoing apoptotic cell death show chromatin condensation and nuclear fragmentation with the appearance of small, apoptotic bodies. The results of these experiments found similar numbers of apoptotic cells in negative controls and the BPV-infected cultures suggesting no virus enhancement of an apoptotic pathway. Staurosporine treatment induced apoptosis in the positive control cultures as expected and there were high numbers of antigen-positive cells detected by IP staining. Further, no significant enhancement of apoptotic body formation was noted in the virus-infected cells. It was thought that if the virus caused death by apoptosis the numbers of apoptotic cells in the virus-infected

cultures would approach the numbers of truly infected cells detected by IP staining. This did not occur as the apoptotic cells in the virus-infected cultures were similar to the negative controls (Fig. 5). These results are indicative of virus-induced cell death by a mechanism other than apoptosis. Because not all markers of apoptosis are positive in cells killed by this mechanism, additional markers of apoptosis were assessed to see if any of them would reveal evidence of apoptotic cell death.

Caspase-activated DNase and other DNases lead to the formation of a nucleosomal ladder by non-random DNA fragmentation. DNA ladders are one of the cardinal signs of apoptotic cells. In this study, cellular DNA from different cell sets was extracted and separated by electrophoresis in 1.5% agarose gel. One of the cell sets used was DMSO treated and that is because staurosporine was dissolved in DMSO. The bands seen in the gel suggested that the control and DMSO treated cells have an intact DNA band and that there was no fragmentation involved. Staurosporine treated cells showed a DNA ladder suggestive of apoptosis. BPV-infected cells have shown DNA fragmentation, but in a random fashion, thus forming smears and small, random bands rather than a ladder. The presence of viral DNA bands is also suspected in the infected cells DNA fragments. Thus, data from this approach support a mechanism of necrotic cell death rather than an apoptotic one (Fig. 7).

Caspases are present in the cells as zymogens. They are activated in apoptotic cells. Thus, caspase staining was used in this study to look for caspase activation. Data from caspase staining indicated that, on average, the number of apoptotic positive cells in the negative control cells and BPV infected cells were approximately the same again

failing to demonstrate apoptosis as a mechanism of cell death in virus infected cells (Fig. 8).

To this point in the study all experiments seeking evidence of apoptosis in virus infected cells failed to provide positive evidence. Therefore, our experiments turned to the search for evidence of necrosis. Cellular morphology is different in each type of cell death. In fact, apoptosis was first identified by the unique cellular morphology changes taking place; such as the formation of apoptotic bodies. In necrotic cell death, cells would swell and then burst; while apoptotic cells do not swell, rather, they shrink and they form apoptotic bodies. Pictures from both synchronized and non-synchronized BPV infected cells do have approximately the same pattern; where cells increase in size followed by cell shrinkage and detachment. No cell division was visualized in infected cells, plus no apoptotic bodies were assessed. Control cells show variation in size with a trend of increased size at the end. This pattern of cell death is more supportive of necrotic cell death rather than apoptotic cell death.

Cells undergoing necrosis release cytoplasmic contents due to bursting. In this study this concept was used to look for necrosis. If BPV infected cells are killed by necrosis then viral proteins and infectious virus particles should be present in the media of cultured cells that are infected with the virus. Infectivity assays and haemagglutination assays were used to search for infectious virus particles and viral proteins in the media, respectively. Data from both assays showed that the number of infectious particles and HA titers increased as CPE increased, which indicated the release of contents from the infected cells to the media (Fig. 19, 20). BPV is not an enveloped virus and does not bud through the membrane of living cells. This virus matures by nuclear assemblage. Thus,

the finding of infectious, cell-released virus in media supernates is suggestive of plasma membrane and nuclear membrane breakdown consistent with cell necrosis. Additionally, the LDH enzyme assay was used to detect cytolysis. The enzyme is a constitutive enzyme present in the cytoplasm of all cell types. When the plasma membrane is damaged due to necrotic burst, LDH is released to the media of cultured cells. The data collected showed that there was more enzyme released into the supernates of BPV infected cells than in the control cells (Fig. 21). Thus, suggesting that there was plasma membrane damage that led to LDH release to the media in the BPV infected culture. This might indicate plasma membrane damage due to the necrosis.

Different approaches were used in this study to look for both apoptotic and necrotic cell death. So far, data from the different approaches used do not support an apoptotic cell death, rather cells become necrotic, they swell, shrink and detach. The detection of cytoplasmic components in the media is also consistent with BPV cell death caused by necrosis.

The model system in the present study employed the permissive cell strain, (EBTr). Non-permissive cells were not studied in this project. Recommendations for future studies would be to perform this research using suitable host cells in which the virus enters but fails to complete the replicative cycle. Perhaps an apoptotic pathway would be triggered in this BPV system similar to that modeled by H-1 virus.

## REFERENCES

1. Abinanti, F.R, M.S. Warfield. 1961. Recovery of a hemadsorbing virus (HADEN) from the gastrointestinal tract of calves. *Virology*. 14:288-289.
2. Brauniger, S., J. Peters, U. Borchers, and M. Kao.2000. Further studies on thermal resistance of bovine parvovirus against moist and dry heat. 203:71-75.
3. Burd, P.R., S. Mitra, R.C. Bates, L.D. Thompson and E.R. Stout. 1983. Distribution of restriction enzyme sites in the bovine parvovirus genome and comparison to other autonomous parvovirus. *J. Gen. Virol.* 64:2521-2526.
4. Chen K., B Shull, E. Moses, M. Lederman, E. Stout, C. Bates. 1986. Complete nucleotide sequence and genome organization of bovine parvovirus. *J.Virol.* 60:1085-1097.
5. Chen, K., B. Shull, M. Lederman, E. Stout, R. Bates. 1988. Analysis of the termini of the DNA of bovine parvovirus: demonstration of sequence inversion at the left terminus and its implication for the replication model. *J. Virol.* 62:3807-3813.
6. Clark, C., S. Boyles. 1999. Possible connection between apoptotic pathways in human parvovirus B19. *Blood Weekly*. P7,1p.
7. Durham, P.J.K., and R.H. Johnson. 1984. Studies on the replication of bovine parvovirus. *Vet. Microbiol.* 10:165-177.
8. Gaddy, D.S., and D.F. Lyles. 2005. Vesicular stomatitis viruses expressing wild- type or mutant M proteins activate apoptosis through distinct pathways. *J. Virol.* 79:4170-4179.
9. Hayder, H.A, J. Storz, and S.Young. 1983. Antigenicity of bovine parvovirus in fetal infections. *Am. J. Vet. Res.* 44:558-563.
10. Hengartner M. 2000. The biochemistry of apoptosis. *Nature*. 407:770-776.
11. Herrmann M., H. Lorenz, R. Voll, W. Woith, and J. Kalden. 1994. A rapid and simple method for the isolation of apoptotic DNA fragments. *Nucleic acid research.* 22:5506-5507.
12. Ikeda Y., J. Shinozuka, T. Miyazawa, K. Kurosawa, Y. Izumiya, Y. Nishimura, K. Nakamura, J. Cai, K. Fujita, K. Doi, T. Mikami. 1998. Apoptosis in feline panleukopenia virus-infected lymphocytes. *J. Virol.* 72:6932-6936.
13. Johnson, F.B, M.D. Hoggan. 1973. Structural proteins of HADEN virus. *Virology.* 51:129-137.

14. Johnson, F.B. 1983. Parvovirus proteins, pp259-295, *In* The parvoviruses, K.I. Berns, Ed., Plenum Press, New York, N.Y.
15. Johnson, F.B, L.B. Fenn, T.J. Owens, L.J. Faucheux, and S.D. Blackburn. 2004. Attachment of bovine parvovirus to sialic acids on bovine cell membranes. *J. Gen. Virol.* 85:2199-2207.
16. Koyama A., T. Fukumori, M. Fujita, H. Irie, and A. Adachi. 2000. Physiological significance of apoptosis in animal virus infection. *Microbes and Infection.* 2:1111-1117.
17. Kopecky S.A., M.C. Willingham, and D.S. Lyles. 2001. Matrix protein and another viral components contribute to induction of apoptosis in cells infected with vesicular stomatitis virus. *J. Virol.*75:12169-12181.
18. Lederman, M., R.C. Bates, and E.R. Stout.1983. In vitro and in vivo studies of bovine parvovirus protein. *J. Virol.* 48:10-17.
19. Li J, E. Werner, M. Hergenahn, R. Poirey, Z. Luo, J. Rommelaere, J. Jauniaux J. 2005. Expression profiling of human hepatoma cells reveals global repression of genes involved in cell proliferation, growth, and apoptosis upon infection with parvovirus H-1. *J. Virol.* 79:2274-2286.
20. Li, P., D. Nijihawan, and X. Wang. 2004. Mitochondrial activation of apoptosis. *Cell.* 116:57-59.
21. Lucas, M.H., and D.G.F Westcott. 1985. Bovine parvovirus. *Vet. Rec.* 116:698.
22. Luker, G., G. Chow, D.F. Richards, and F.B. Johnson. 1991. Suitability of infection of cells in suspension for detection of herpes simplex virus. *J. Clin. Microbiol.* 29:1554-1557.
23. Moehler M., B. Blechacz, N. Weiskopf, M. Zeidler, W. Stremmel, J. Rommelaere, P. Galle, and J. Cornelis. 2001. Effective infection, apoptotic cell killing and gene transfer of human hepatoma cells but not primary hepatocytes by parvovirus H1 and derived vectors. *Cancer Gene Therapy.* 8:158-167.
24. Moffatt S., N. Yaegashi, K. Tada and K. Sugamura. 1998. Human parvovirus B19 nonstructural (NS1) protein induces apoptosis in erythroid lineage cells. *J. Virol.* 46:3574-3579.
25. Monteith, H.D., E.E. Shannon, and J.B. Derbyshire. 1986. The inactivation of a bovine enterovirus and a bovine parvovirus in cattle manure by anaerobic digestion, heat treatment, gamma irradiation, ensilage and composting. *J. Hyg.* 97:175-184.

26. Ohshima T., M. Iwama, Y. Ueno, F. Sugiyama, T. Nakajima, A. Fukamizu and K. Yagami. 1998. Induction of apoptosis in vitro and in vivo by H-1 parvovirus infection. *J. Gen. Virol.* 79:3067-3071.
27. Raj, K., P. Ogston, and P. Beard. 2002. Virus-mediated killing of cells that lack p53 activity. *Nature.* 412:914-917.
28. Sandals, W.C., R.C. Poverly, and A.H. Meek. 1995. Prevalence of bovine parvovirus infection in Ontario dairy cattle. *Can. J. Vet. Res.* 59:81-86.
29. Selliah, N. and T.H. Finkel. 2001. Biochemical mechanisms of HIV induced T cell apoptosis. *Nature.* 8:127-136.
30. Shen Y, and T. Shenk. Viruses and apoptosis. 1995. *Current opinion in genetics and development.* 5:105-111.
31. Storz, J., R.C Bates, G.S. Warren, and T.H. Howard. 1972. Distribution of antibodies against bovine parvovirus 1 in cattle and other animal species. *Am. J. Vet. Res.* 33:269-272.
32. Stortz J., and R.C. Bates. 1973. Parvovirus infections in calves. *J. Am. Vet. Med. Assoc.* 163:884-886.
33. Thacker, T.C and F.B. Johnson. 1998. Binding of bovine parvovirus to erythrocyte membrane sialylglycoproteins. *J. Gen. Virol.* 79:2163-2169.
34. Yaun, J., and R. Horvitz. 2004. A first insight into the molecular mechanism of apoptosis. *Cell.* 116:53-56.